Masters Theses   Graduate School

12-1991

Solidification kinetics of alpha versus gamma formation of aluminum oxide (Al2O3) particles in solid propellant rocket exhausts : an analytical approach

Suzanne Moore Oliver

Follow this and additional works at: https://trace.tennessee.edu/utk_gradthes

To the Graduate Council:

I am submitting herewith a thesis written by Suzanne Moore Oliver entitled "Solidification kinetics of alpha versus gamma formation of aluminum oxide (Al2O3) particles in solid propellant rocket exhausts : an analytical approach." I have examined the final electronic copy of this thesis for form and content and recommend that it be accepted in partial fulfillment of the requirements for the degree of Master of Science, with a major in Mechanical Engineering.

Rober Crawford, Major Professor

We have read this thesis and recommend its acceptance:

Wheeler McGregor, Mary Helen McCay, Roy Schulz
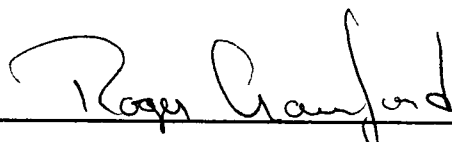
Accepted for the Council:

Carolyn R. Hodges

Vice Provost and Dean of the Graduate School

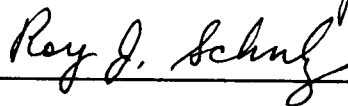(Original signatures are on file with official student records.)
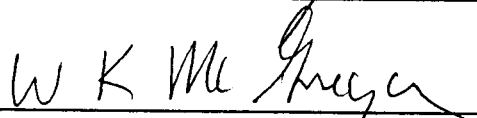
To the Graduate Council:

I am submitting herewith a thesis written by Suzanne Moore Oliver entitled "Solidification Kinetics of Alpha Versus Gamma Formation of Aluminum Oxide (Al_2O_3) Particles in Solid Propellant Rocket Exhausts: An Analytical Approach." I have examined the final copy of this thesis for form and content and recommend that it be accepted in partial fulfillment of the requirements for the degree of Master of Science, with a major in Mechanical Engineering.

_____
Dr. Roger Crawford, Major Professor

We have read this thesis
and recommend its acceptance:

_____

_____

_____

Accepted for the Council:

_____
Associate Vice Chancellor
and Dean of the Graduate School

STATEMENT OF PERMISSION TO USE

In presenting this thesis in partial fulfillment of the requirements for a Master's degree at The University of Tennessee, Knoxville, I agree that the Library shall make it available to borrowers under rules of the Library. Brief quotations from this thesis are allowable without special permission, provided that accurate acknowledgment of the source is made.

Permission for extensive quotation from or reproduction of this thesis may be granted by my major professor, or in his absence, by the Head of Interlibrary Services when, in the opinion of either, the proposed use of the material is for scholarly purposes. Any copying or use of the material in this thesis for financial gain shall not be allowed without my written permission.

Signature _S. M. Oliver_

Date _11/19/91_

SOLIDIFICATION KINETICS OF ALPHA VERSUS GAMMA FORMATION OF ALUMINUM OXIDE (Al_2O_3) PARTICLES IN SOLID PROPELLANT ROCKET EXHAUSTS: AN ANALYTICAL APPROACH

A Thesis

Presented for the

Master of Science

Degree

The University of Tennessee, Knoxville

Suzanne Moore Oliver

December 1991

ACKNOWLEDGEMENTS

ABSTRACT

The objective of this research was to provide insight into the solidification kinetics of aluminum oxide (Al_2O_3) particles formed in the exhaust of solid rocket motors (SRM) which use aluminized propellants. The research was motivated by the observation that particles collected from SRM exhausts often show more than one crystalline phase of Al_2O_3. The larger particles tend to be composed of the stable alpha phase while the smaller particles tend to be composed of gamma or one of the other metastable phases. The various phases of Al_2O_3 have different properties and crystalline structures. The existence of multiple phases is important in applications where particle density, chemical properties, and optical properties need to be considered. It is not important to motor performance since the enthalpy difference between the phases is insignificant.

Although much is known in the field of ceramics about the solidification kinetics of Al_2O_3, this knowledge had not been applied to rocket exhaust products in a systematic manner. Thus, an analytical method was devised which combined the solidification kinetics of Al_2O_3 and the output from industry standard nozzle and plume codes. This method was used to investigate the dependence of the crystal phase of solid Al_2O_3 particles upon various parameters.

The kinetic rate analysis indicates that the rapid temperature quench occurring in a gas dynamic nozzle expansion and free expansion into the atmosphere is capable of producing significant amounts of metastable aluminas. It also shows a direct correlation between crystal phase and particle size, the degree of undercooling, motor type, and altitude.

TABLE OF CONTENTS

LIST OF FIGURES

NOMENCLATURE

A	Frequency factor
ASRM	Advanced Solid Rocket Motor
Al_2O_3	Aluminum oxide
$AlCl_3$	Aluminum chloride
B	Reactant
C	Reactant
CEC	Chemical Equilibrium Code
Cr	Chromium
Cr_2O_3	Chromium (III) oxide
df/dt	Rate (or slope) of the reaction
f	Solid mass fraction of gamma
fcc	Face centered cubic
Fe	Iron
HCl	Hydrogen Chloride
hcp	Hexagonal close pack
HPM	High-Performance Motor
HTPB	Hydroxy-terminated polybutadiene
k	Reaction rate
K	Kelvin
m	Rate exponent for reactant B
n	Rate exponent for reactant C
O_3	Ozone

PBAN	Polybutadiene acrylonitrile
Pc	Motor chamber pressure, psia
Q	Activation Energy
r	Rate constant
R	Gas constant
RAMP	Reacting and Multi-Phase Code
Re	Nozzle exit radius
RSRM	Redesigned Solid Rocket Motor
SPF/2	Standard Plume Flowfield Code (Version 2)
SPP	The Solid Propellant Rocket Motor Performance Prediction Computer Program
SRM	Solid Rocket Motor
T1	Gas Temperature before the shock (or reflection)
t	Time, sec
T	Temperature, K
Tsolidification	Al_2O_3 solidification temperature, K
TiO_2	Titanium dioxide
Tmax	Maximum gas temperature, K
Tmelt	Al_2O_3 melt temperature, K
X	Axial distance from nozzle exit
ΔT	Change in gas temperature due to Mach disc (or reflection)
μm	Micron

CHAPTER I.

INTRODUCTION

Most of the solid rocket propellants in use today utilize a polymer matrix which contains powdered aluminum. A primary effluent from the exhausts of solid rocket motors (SRM) which use these aluminized propellants is particulate aluminum oxide (Al_2O_3). The formation of Al_2O_3 (or alumina) occurs in the motor chamber (Fig. 1) during combustion of the fuel at temperatures higher than the Al_2O_3 melt point. Some of the liquid Al_2O_3 droplets are broken up by the strong shear forces encountered as the nozzle flow accelerates through the nozzle throat. The rocket exhaust expands downstream of the nozzle throat, and the alumina eventually solidify as the temperatures of the gas and the Al_2O_3 continue to decrease. If the cooling rate of the exhaust is sufficiently fast, the droplets may reach a temperature lower than the melt temperature (i.e. undercool) before solidification occurs.

Samples collected from SRM exhausts have shown that the alumina sometimes exists in more than one crystalline phase [1,2]. The most thermodynamically stable phase of Al_2O_3 is the alpha crystalline phase. Several other less stable phases exist which include the eta, gamma, delta, theta, chi, and kappa phases [3]. Although other crystalline phases may be present, the smaller particles are primarily composed of the metastable gamma phase while the larger particles are predominantly the stable alpha phase [4].

a. Solid Rocket Motor

b. Plume and Particle Streamlines
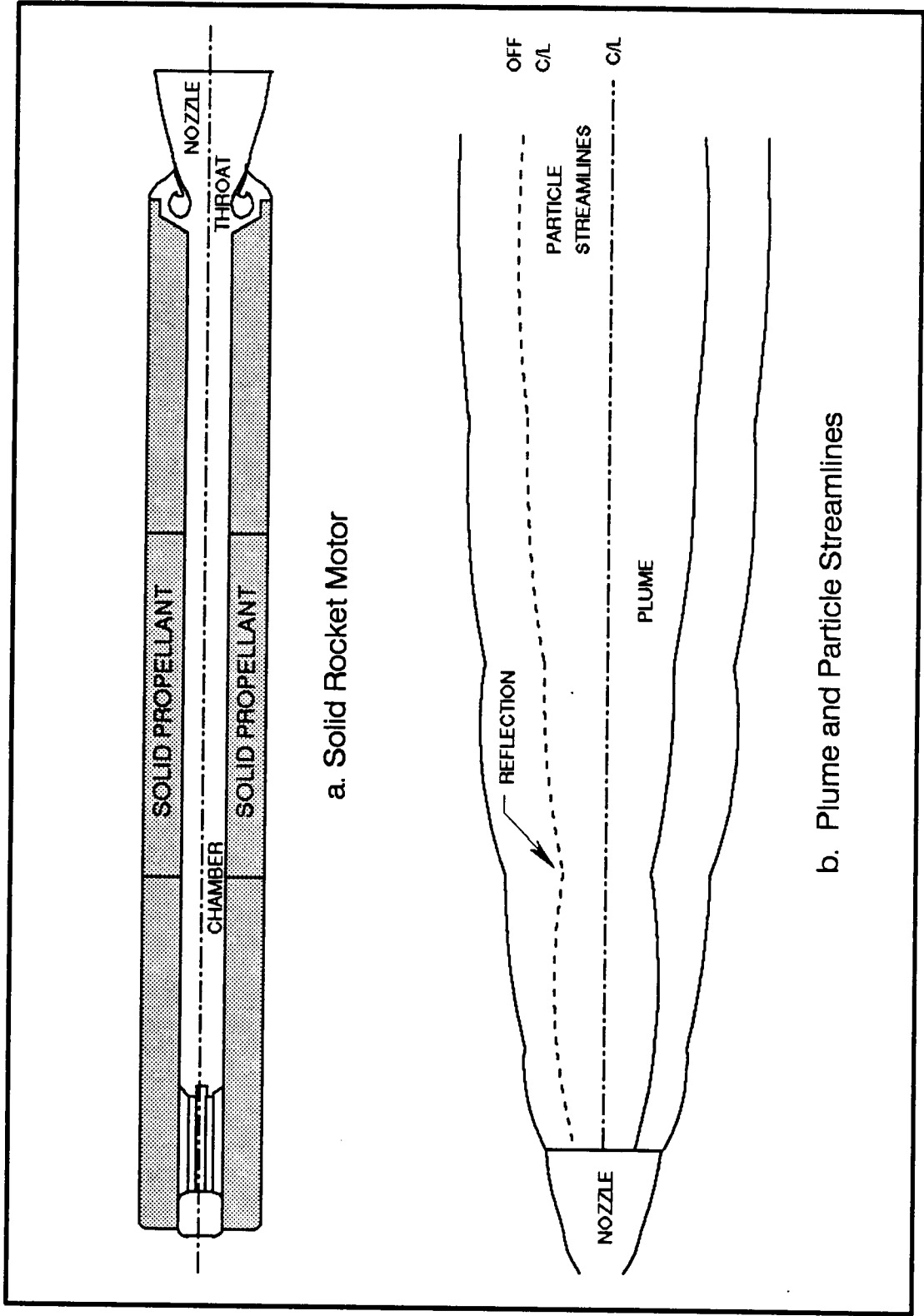
Figure 1. Sketch of Solid Rocket Motor and Particle Streamlines

2

The alpha and gamma phases of alumina have different crystalline structures and properties as shown in Table 1. These differences are not important in terms of motor performance (i.e. thrust, specific impulse, etc.) due to the small variations in enthalpy between the phases. However, the existence of metastable phases in the rocket exhausts should be considered in applications where particle density, chemical properties, or optical properties are important.

One example of the importance of the optical properties of the different alumina phases is in the measurement of particle size using laser techniques. The difference in refractive indices (Table 1) between the alpha and gamma phases of Al_2O_3 can correspond to a factor of two difference in the backscatter cross section. This can adversely affect the particle size measurements which are required in the determination of two-phase motor performance loss and in the calculation of the radiative heat transfer from the plume [5].

Another phase dependent property of alumina which may affect the accurate calculation of plume radiative heating is the particle emissivity. The smaller electronic band gap value [6] for the gamma phase (Table 1) implies that gamma phase alumina may have a higher emissivity than the alpha phase. This could be one reason why the measured values of the radiative heating from the plumes exhausted from space motors are usually higher than predicted values [5]. Also, the difference in the absorption spectra of the gamma and alpha phases has

Table 1. Physical Properties of Alpha and Gamma Al_2O_3

Property[1]	Alpha	Gamma
Density, g/cc	3.98	3.6
Free Energy, kcal/mole	-397.594	-396
Oxygen Sublattice	hexagonal (hcp)	cubic (fcc)
Melting Point, K	2327	2289
Heat of Fusion, cal/g	256	122
Band Gap, eV	8.8	7.2
Visible Refractive Index	1.78	1.65 (approx)
Solubility	insoluble in acids and bases	slightly soluble

[1] Properties given at room temperature

been suggested and has been partly evaluated as a method of discerning the mass fraction of the gamma and the alpha phases in particle sample collections [4].

The question of the environmental impact of the space shuttle exhaust is one example where the chemical properties of the alumina phases may be of importance. Of all the current launch vehicles, the space shuttle releases the most exhaust products in a single launch [7]. Approximately 276,000 kg of the shuttle SRM exhaust effluents released into the atmosphere consist of Al_2O_3 [2]. Most of the Al_2O_3 (about 63 percent) exhausted by the shuttle is released into the troposphere (altitudes up to approximately 15 km or 50,000 ft). The remaining effluent is deposited in the stratosphere up to an altitude of about 43 km (about 140,000 ft) [2, 7]. A few gamma phase particles have been collected from the shuttle contrail at low altitudes [2], but very little is known about the relative amount of alpha or gamma phase particles exhausted into the stratosphere.

The gamma phase particles are more chemically reactive than the alpha phase particles and can form toxic aluminum chloride ($AlCl_3$) hydrate (an irritant to eyes and mucous membranes) from the hydrogen chloride (HCl) and H_2O in the shuttle launch cloud [8] as shown in equation 1 [9].

$$Al_2O_3(s) + 6HCl(g) + 9H_2O(g) \rightarrow 2[AlCl_3 * 6H_2O](s) \qquad (1)$$
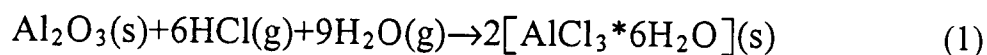
The particulate gamma phase alumina may serve as nucleation sites on which HCl can condense and eventually increase acidity at ground level [8]. The possibility of the gamma phase particles acting as an ice nucleation agent in the

5

upper troposphere and lower stratosphere has also caused some environmental concerns in terms of possible climatic impact [2, 10]. Although recent studies indicate that this may not be a viable issue [11], the long term environmental impact of the exhausted alumina cannot be known until the amount of the metastable crystalline phases have been determined.

Thus, the solid rocket motors used on the space shuttle are of particular utility in the study of solidification kinetics of Al_2O_3 particles. The Redesigned Solid Rocket Motor (RSRM) is the shuttle SRM currently in use. An Advanced Solid Rocket Motor (ARSM) is being developed which will eventually replace the RSRM. The current shuttle SRM (the RSRM) has a 16 percent aluminum loading. However, the aluminum loading will be increased to 19 percent for the ASRM. The increase in thrust provided by the ASRM will allow an increase in shuttle payload capacity. However, the increased thrust translates into an increase in liquid alumina in the near field plume. This results in a higher plume radiance. It has been predicted that the plume radiance of the ASRM may be as much as 75 percent higher than the plume radiance of the RSRM. [12].

An analytical approach was developed in this work which utilized the flowfield output provided by Moylan [12,13] and current kinetic rate information on Al_2O_3 [14] to calculate the amount of gamma retention in the ASRM and RSRM plumes under various conditions. The particle temperatures and velocities provided from Moylan's flowfield calculations were input into a phase conversion

6

code which used Steiner's [14] global kinetic rate equation to estimate the amount of gamma to alpha conversion. Sixty different cases were considered which varied such parameters as particle size, undercooling, motor type, and altitude. The results of these calculations are presented and discussed in this thesis.

CHAPTER II.

BACKGROUND

Crystal Phase

Aluminum oxide occurs in several forms in nature. In the hydrated form it occurs as bauxite, and in the anhydrous form it occurs as corundum. Commercially, some forms of corundum are used as abrasives while other forms are valued as gemstones. The gemstones are formed as a result of impurities in the corundum due to various metallic oxides (for example, the impurities of chromium (III) oxide (Cr_2O_3) and titanium dioxide (TiO_2) result in the gemstones known as rubies and sapphires, respectively). However, although the various forms of aluminum oxide have the same formula, Al_2O_3, they have different crystalline structures and thus different properties [15].

Corundum, or alpha phase Al_2O_3, is the most stable crystalline form exhibited by aluminum oxide. The alpha crystalline structure consists of hexagonal close packed (hcp) oxygen anions with two thirds of the octahedral interstices occupied by aluminum cations [3, 16]. Fig. 2a shows a diagram of the corundum structure with one-third of the possible aluminum sites vacant [17].

There are numerous metastable crystalline phases of solid alumina which also exist in addition to the stable alpha phase. These less stable phases are classified into two major groups: the alpha series and the gamma series. The oxygen anions of the alpha series are hexagonal close packed (as in corundum)
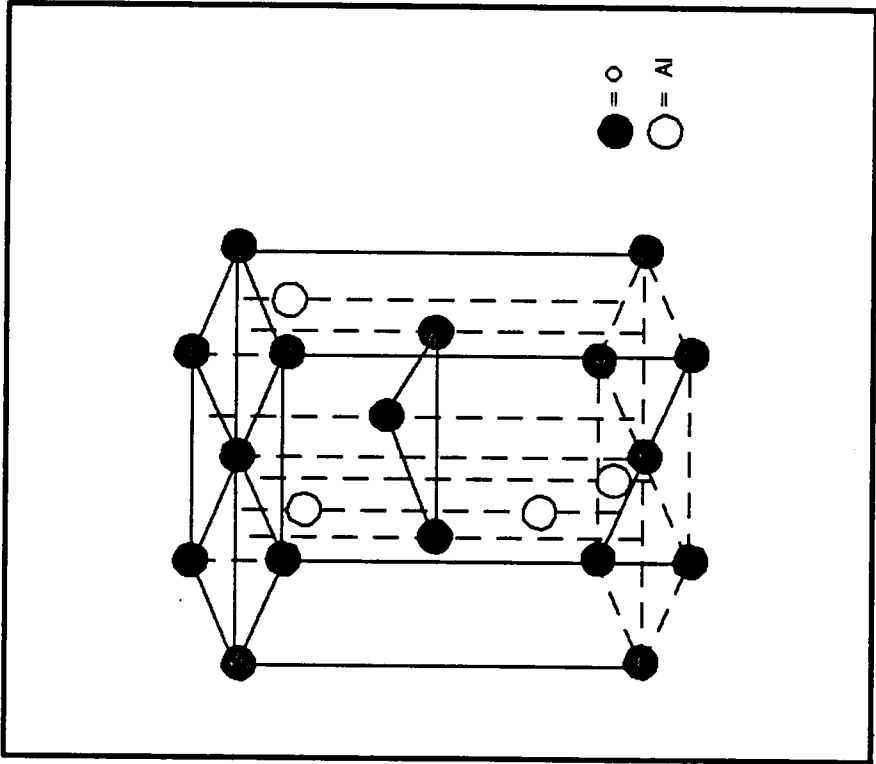
a. Alpha Phase (Corundum)
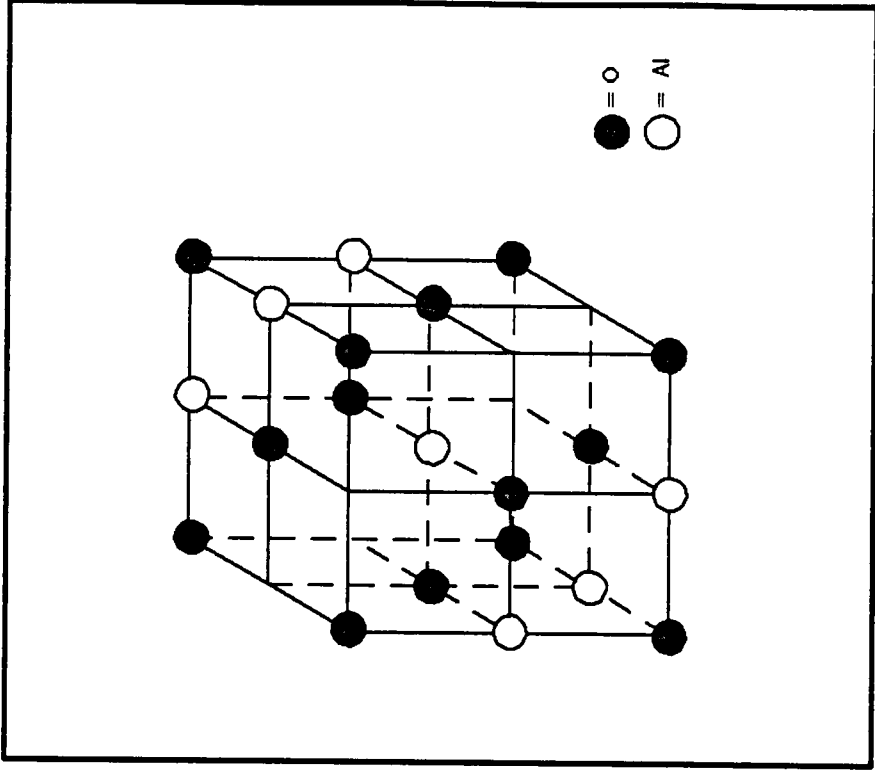
b. Gamma Phase (Spinel)

Figure 2. Diagram of Alumina Crystalline Structure

9

while those of the gamma series are face centered cubic (fcc, characteristic of spinel) as shown in Fig. 2b. The alpha series typically consists of the chi and kappa phases while the gamma series includes eta, gamma, delta, and theta. The differences between the phases within each series are due to the variations in the cation sublattice arrangement [3].

All the metastable phases eventually transform into the stable alpha phase provided they remain at elevated temperatures for a sufficient length of time. When the liquid Al_2O_3 solidifies, it is most likely to evolve into gamma. Then, if there is sufficient time, it may progress through other phases (delta and theta) until it finally transforms into the alpha phase with the final transformation requiring the rearrangement of the anion sublattice. Phase selection as a function of particle size has been reported by Levi [3] during an investigation in which electrohydrodynamic atomization was applied in order to produce Al_2O_3 droplets ranging from 10 nm to 300 μm in size. His study revealed that a diversity in microstructures were exhibited in the particles ranging from amorphous Al_2O_3 to corundum as shown in Table 2 [3].

The two main crystalline phases of Al_2O_3 which have been observed in samples collected from SRM exhausts are the stable alpha phase and the metastable gamma phase. Not only are these two phases different in structure, but they also exhibit different properties as shown in Table 1. The existence of these two phases in SRM exhausts have little effect in terms of motor performance since

Table 2. Phase Selection as Function of Particle Size

Crystal Phase	Particle Diameter, μm				
	0.01	0.10	1.0	10	100
Amorphous	←----------------------				
Gamma		--			
Delta, Theta				---------------	
Alpha				------------------→	

the difference in enthalpy is relatively small. However, the presence of multiphases may be important in applications in which the optical properties, chemical properties, or density of the exhaust must be considered.

Kinetic Rate

An increase in temperature usually increases the rate of a chemical reaction. In 1889, Arrhenius discovered that an equation with the same form as the Van't Hoff isochore could account for the effect of temperature on the reaction rate in most cases [18]. This equation (known as the Arrhenius equation or Arrhenius Law) can be deduced from the Law of Mass Action and the Van't Hoff equation, and is usually written in its integrated form as follows [18]:

$$k = A * e^{\frac{-Q}{RT}} \tag{2}$$

where   k = Specific reaction rate (or velocity constant)

A = Frequency factor (integration constant)

Q = Activation energy of the reaction

R = Gas constant

T = Temperature

The frequency factor is related to the frequency of the collisions of the reacting molecules and their orientation. That is, it indicates the number of collisions with the proper orientation for reaction [9]. The exponential factor $e^{-Q/RT}$ indicates the fraction of the molecules that have an energy greater than or equal to

12

the activation energy of the reaction [9, 18]. The activation energy is the minimum energy required to form a transition state during the collision between reactants. The concept of activation energy is illustrated in Fig. 3. There is a natural tendency for the molecules in a system to take positions such that the energy is at a minimum. However, there is often an energy barrier which must be overcome before this can occur. The energy which must be put into a system in order to overcome the energy barrier is known as the activation energy [9].

The order of the reaction indicates the number of reacting species (i.e. atoms or molecules) involved whose concentrations determine the kinetics of the reaction, and it is equal to the sum of the concentration terms of the reactants in the rate of reaction equation [18]. The order can be expressed in terms of each reactant or with respect to the overall order of the reaction. For example, in the general rate equation

$$k=r[B]^m[C]^n \tag{3}$$

r is a rate constant and B and C are two reactants. If the exponent m is equal to 1, then the reaction is said to be first order with respect to B. If the exponent n is equal to 2, the reaction is said to be second order with respect to C. The overall rate of the reaction is equal to the sum of the orders of each reaction (m + n). In this case, the overall reaction is third order (1 + 2). If a reaction is zero order, the rate of the reaction is constant and does not change with time (i.e. the rate does not change with reactant concentration). Thus, if the extent of the reaction, f, is

13
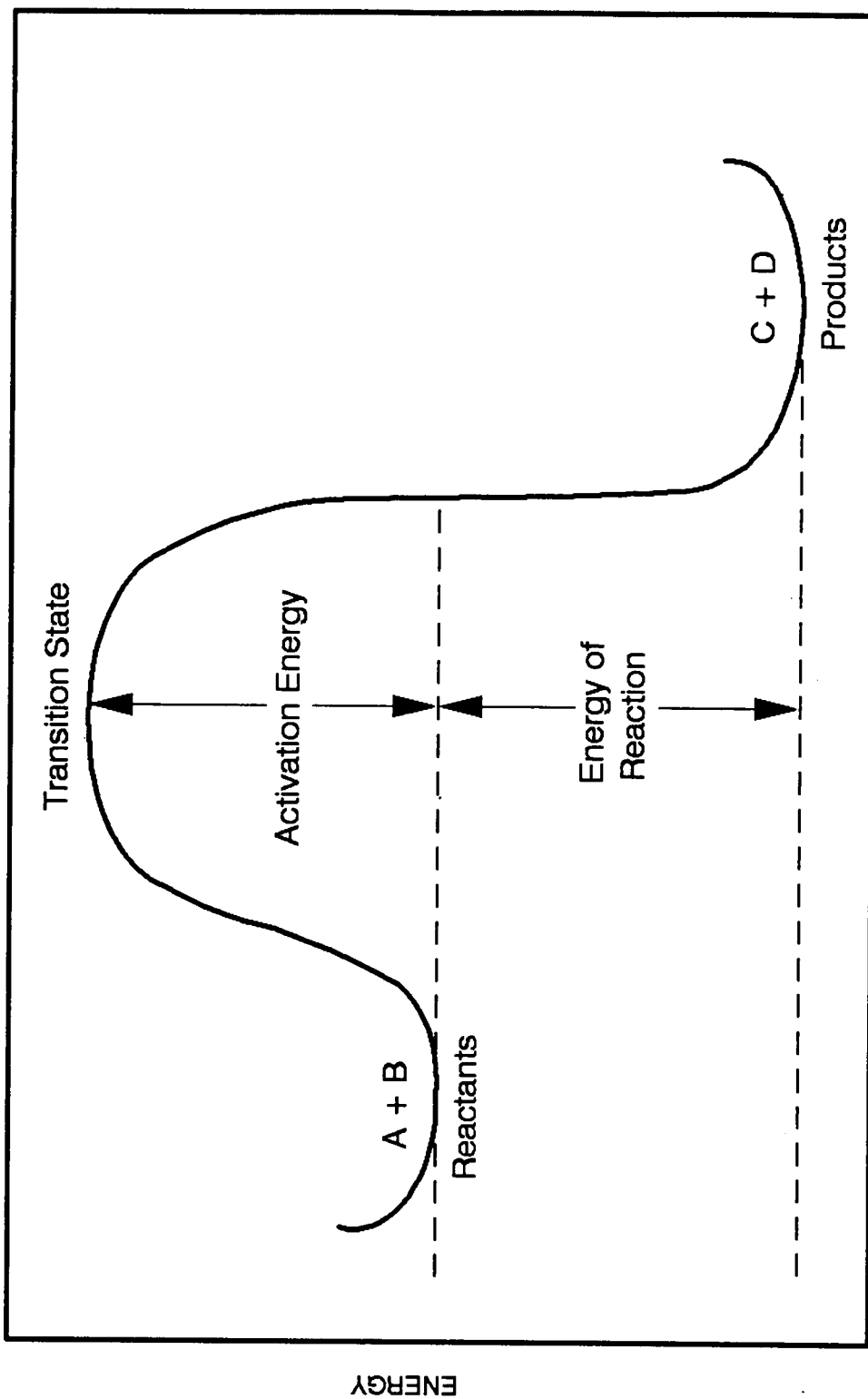
Figure 3.   Illustration of Activation Energy

14

plotted as a function of time, t, the result will be a straight line, and the rate of the reaction, k, is given by the slope df/dt [9, 18]:

$$\frac{df}{dt} = k \qquad (4)$$

The global reaction rate for the conversion of gamma to alpha in uncompacted aluminum powders has been determined during several studies in which the transformation of gamma to alpha followed first order kinetics. The activation energies found ranged from 79 to 153 kcal/mol [14, 19-22].

One of the most comprehensive rate studies was performed by Steiner et al. [14] using a starting material of high purity gamma Al_2O_3 powder. The activation energy determined by Steiner was 116 kcal/mol. This value was confirmed by Kato et al. [19] in a study which used an alumina powder starting material prepared from hydrated aluminum sulfate. Steiner's results indicated that the transformation followed zero order kinetics (m=n=0). This zero order rate constant with an Arrhenius temperature dependence can be express as follows [3, 14]:

$$k = \frac{df}{dt} = 1.7E14 * e^{\frac{-58368}{T}} \quad \text{(per sec)} \qquad (5)$$

where   f = the fraction of alpha Al_2O_3

             k = the rate constant

             t = time, sec

             T = temperature, K

Since the relative rates of the intermediate phases from gamma to alpha have not been determined, it was assumed for this study that the transformation occurred directly from gamma to alpha [3].

Although Steiner obtained good results using alumina powder of high purity, it has been observed that different types of impurities can greatly affect the phase transformations by either accelerating or retarding the reaction [3, 20]. For example, the addition of chromium (Cr) to amorphous aluminum hydroxide caused a reduction in the conversion rate by a factor of two while the addition of iron (Fe) increased the rate in a study performed by Bye and Simpkin [19, 20].

Thus, although rate equations for the conversion of gamma to alpha have been determined for pure alumina powders, the direct application of these equations to calculations involving contaminated alumina (i.e. from rocket exhausts) introduces an unknown margin of error. For example, if the rate equation developed by Steiner is increased or decreased by a factor of two, the amount of alpha conversion is increased or decreased by roughly a factor of two. However, until a rate equation is determined from a study which uses alumina obtained from rocket exhausts, Steiner's rate equation provides a first estimate of the amount of metastable alumina that may be produced in a SRM exhaust.

Shuttle Solid Rocket Motors

The first space shuttle SRM was developed during the mid-1970s, and the first shuttle was launched in April 1981. The High-Performance Motor (HPM) was

16

designed in the early 1980s to increase motor performance [23]. In mid-1986, the design was begun on a new SRM referred to as the Redesigned Solid Rocket Motor (RSRM). The launch of the Discovery shuttle on September 29, 1988 marked the first flight of a shuttle configured with the RSRM [23]. An Advanced Solid Rocket Motor (ASRM) with increased thrust is currently being developed which will increase the shuttle payload capacity.

The overall dimensions of the RSRM and ASRM are approximately equivalent with an overall length of 1,513 in. and an nozzle exit diam of about 150 in. (Table 3) [24]. The RSRM (manufactured by Thiokol Corp.) consists of four segments designed to provide thrust to the shuttle from liftoff until the first 123 sec of flight. The ASRM (manufactured by Lockheed Missiles and Space Company) consists of three segments designed to provide thrust to the shuttle from liftoff until the first 134 sec of flight [24]. The fuel used in the RSRM is polybutadiene acrylonitrile (PBAN) with a 16 percent aluminum loading [23]. The ASRM will use hydroxy-terminated polybutadiene (HTPB) with an aluminum loading of 19 percent [24]. The additional aluminum in the ASRM fuel results in an increase in gas temperature which provides increased thrust and payload capacity. However, the increase in gas temperature translates into an increase in liquid alumina in the nearfield plume. This results in a higher plume radiance which may be as much as 75 percent higher than the RSRM plume radiance according to predictions [12].

Table 3. RSRM and ASRM Design Parameters

Parameters	RSRM	ASRM
Total Length, in.	1,513	1,513
Case Diameter, in.	146	150
Nozzle Exit Radius, in.	74.8	74.8
Nozzle Throat Radius, in.	26.92	26.89
Area Ratio (Ae/At)	7.72	7.74
Average Chamber Pressure, psia	625	633
Avg. Vacuum Thrust, lbf (webb time)	2,590,000	2,624,031
Specific Impulse, sec (Vacuum)	267.9	270.3
Motor Weight, lbs	1,255,978	1,345,807
Propellant Weight, lbs	1,107,169	1,205,807
Propellant Type	PBAN	HTPB
Aluminum Loading, %	16	19
Burn Rate, in/sec (@ 625 psia)	0.368	0.345

Source: Bardos, R., "Shuttle Propulsion Systems," *Space Transportation Propulsion Technology Symposium, Vol. 2 - Symposium Proceedings,* NASA CP-3112, Vol. 2, pp.151-166, May 1991.

CHAPTER III.

METHODOLOGY

Introduction

Preliminary calculations were previously performed to determine the gamma to alpha conversion for one-dimensional, isentropic flow expanding in a conical nozzle [5]. The motors considered in that study were smaller than the ASRM and RSRM with throat radii of 3.94 in. (about 10 cm) or less and thrusts of approximately 100,000 lbf. A computer code was developed which integrated three coupled differential equations consisting of the alumina velocity, enthalpy, and crystal phase. The methodology that was used to calculate the momentum and heat transfer was comparable to those used in the Solid Propellant Performance (SPP) code [25] and the Standard Plume Flowfield (SPF) code [12,13].

The one-dimensional study suggested that significant amounts of metastable alumina may be formed in solid rocket motors which use aluminized propellants. The code developed in this study was limited to motors with low aluminum loading since the assumption of one-dimensional, isentropic expansion did not allow for two-phase coupling between the gas and the condensed phase. Thus, another methodology was needed which would provide insight into the gamma to alpha conversion for the aluminum loadings commonly used in solid-propellant rocket motors.

An analytical approach was developed in the current study which utilized the flowfield output from industry standard nozzle and plume codes as input into a phase conversion code which predicted the amount of gamma to alpha conversion in SRM exhausts. The various components in this methodology are described in the following sections.

Standard Nozzle and Plume Codes

Since the environmental impact of the space shuttle exhaust continues to be of interest, the ASRM and RSRM were selected for this study. Also, these motors were larger (throat radius of 26.8 in. and thrust greater than 2,500,000 lbf) than the motors studied in the one-dimensional analysis and provided additional insight into the importance of motor size in the formation of metastable alumina in SRM exhausts.

Initial plume predictions had already been performed on these motors by Moylan [12] using three industry standard nozzle and plume codes. Additional calculations were provided by Moylan as input for the current analysis.

The first prediction code used by Moylan was the Chemical Equilibrium Code (CEC) [26]. The input for this code (propellant composition and motor operating pressure) was supplied by SECA Inc. [27]. CEC was used to calculate the gas constituents at the throat of the nozzle assuming chemical equilibrium. The output from this code (combustion temperature and exhaust gaseous species percent mole fractions) was used as input to the second prediction code.

The Reacting and Multi-Phase Code (RAMP) [12] was used to calculate the nozzle flowfield properties. The nozzle exit plane startline conditions generated with RAMP were used as input to the third code, the Standard Plume Flowfield Code (SPF/2) [12, 13] .

The SPF code was used to predict the entire chemically reacting plume flow field from the nozzle exit plane to the far field with an output of the gas static properties, particle properties, and the domain of the Mach disc or reflection point with an assumption of two phase non-equilibrium.

An undercooling (or supercooling) option, which Moylan incorporated into the SPF/2 code, was also used to calculate particle temperatures and velocities for various degrees of undercooling. In the undercooling option, the solidification temperature of the alumina was assumed to have a value ranging from 80 to 95 percent of the Al_2O_3 melt temperature in order to calculate particle undercooling ranging from 20 to 5 percent, respectively. No particle undercooling was assumed whenever the solidification temperature was equal to the melt temperature. The melt temperature assumed in the code calculations was 2318 K. This value is in between the temperatures listed in Table 1 for the alpha and gamma phases. The five particle groupings selected by Moylan for these calculations ranged in size from 3.5 to 9.1 μm in radius. These particle sizes were selected based on experimental data acquired from similar motors with similar propellants and

21

operating conditions. The methodology which Moylan used in performing the nozzle and plume flowfield calculations are described in more detail in Ref. 12.

Gamma to Alpha Conversion Code

A gamma to alpha conversion code was developed by the author of the present thesis which integrated the Steiner kinetic rate equation (equation 5) by using Simpson's Rule. The particle temperatures and velocities at various axial locations were calculated using SPF/2 (flowfield output provided by Moylan on floppy diskettes) and used as inputs to this code. However, these inputs were not provided at evenly spaced increments and thus had to be interpolated at even axial locations in order to be used in the conversion code. This required the development of an additional code which could interpolate up to twelve numbers for a given axial location.

The interpolation code was used to calculate the particle temperature and velocity for five particle sizes at 6 in. increments for distances ranging from 0 to 780 ft (125 nozzle radii) downstream of the nozzle exit. In addition to calculating the properties at evenly spaced increments, the interpolation code was used to determine the axial location at which each particle size solidified. For the cases in which undercooling was considered, the location at which the particles reached the solidification temperature also had to be determined. The results from this code were written to separate files for use in the phase conversion code.

CHAPTER IV

RESULTS

Temperature-Time Histories

The temperature-time histories (calculated using the nozzle codes and SPF/2) for Al_2O_3 particles of various sizes at an altitude of 100,000 ft and without undercooling are shown in Figs. 4-6. Calculations were made for the ASRM on centerline (Fig. 4) and off centerline (Fig. 5). The RSRM on-centerline calculations are shown in Fig. 6. As shown in Fig. 1, the on-centerline calculations were made on a line corresponding to the motor centerline. The off-centerline calculations were made on a line which corresponded to the 25th radial grid location from the centerline in the SPF/2 flow field (50 radial grid locations were used to define the flow field). These calculations were made without allowing the particles to undercool (i.e. the particles were treated as solid below a temperature of 2318 K); however, additional calculations were made in which the degree of particle undercooling was varied.

In these figures, the ordinate is the temperature of the Al_2O_3 particles and the gas in Kelvin. The lower abscissa is a dimensionless axial distance given by the ratio of the distance (X) of the particles and the gas downstream of the nozzle exit to the radius of the nozzle exit (Re). The upper abscissa is the approximate elapsed time (in sec) from the time the particles and gas left the nozzle exit until they reached an axial location downstream of the nozzle which corresponds to a
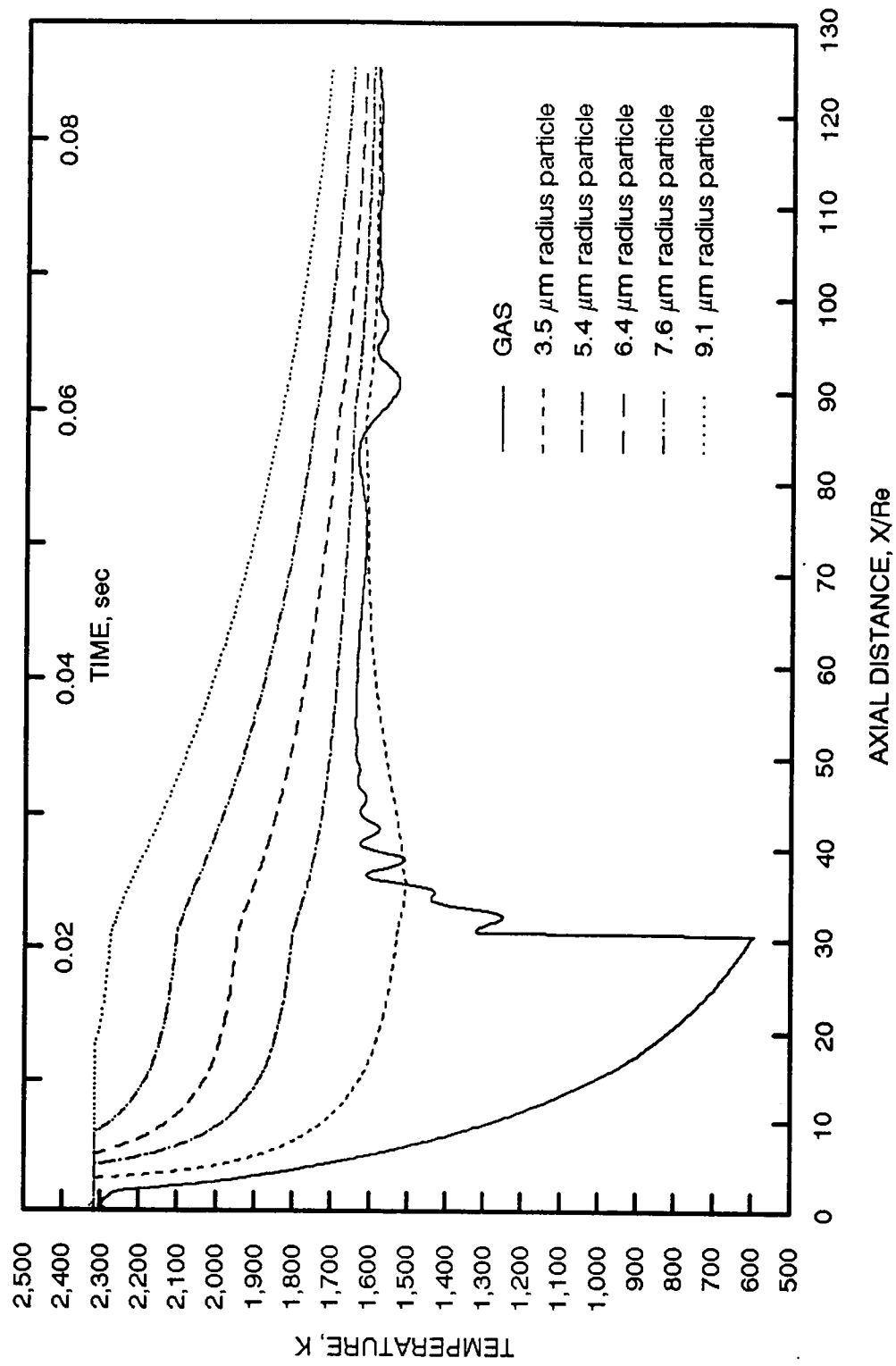
Figure 4. ASRM Temperature Profiles at 100,000 ft, On Centerline, Without Undercooling
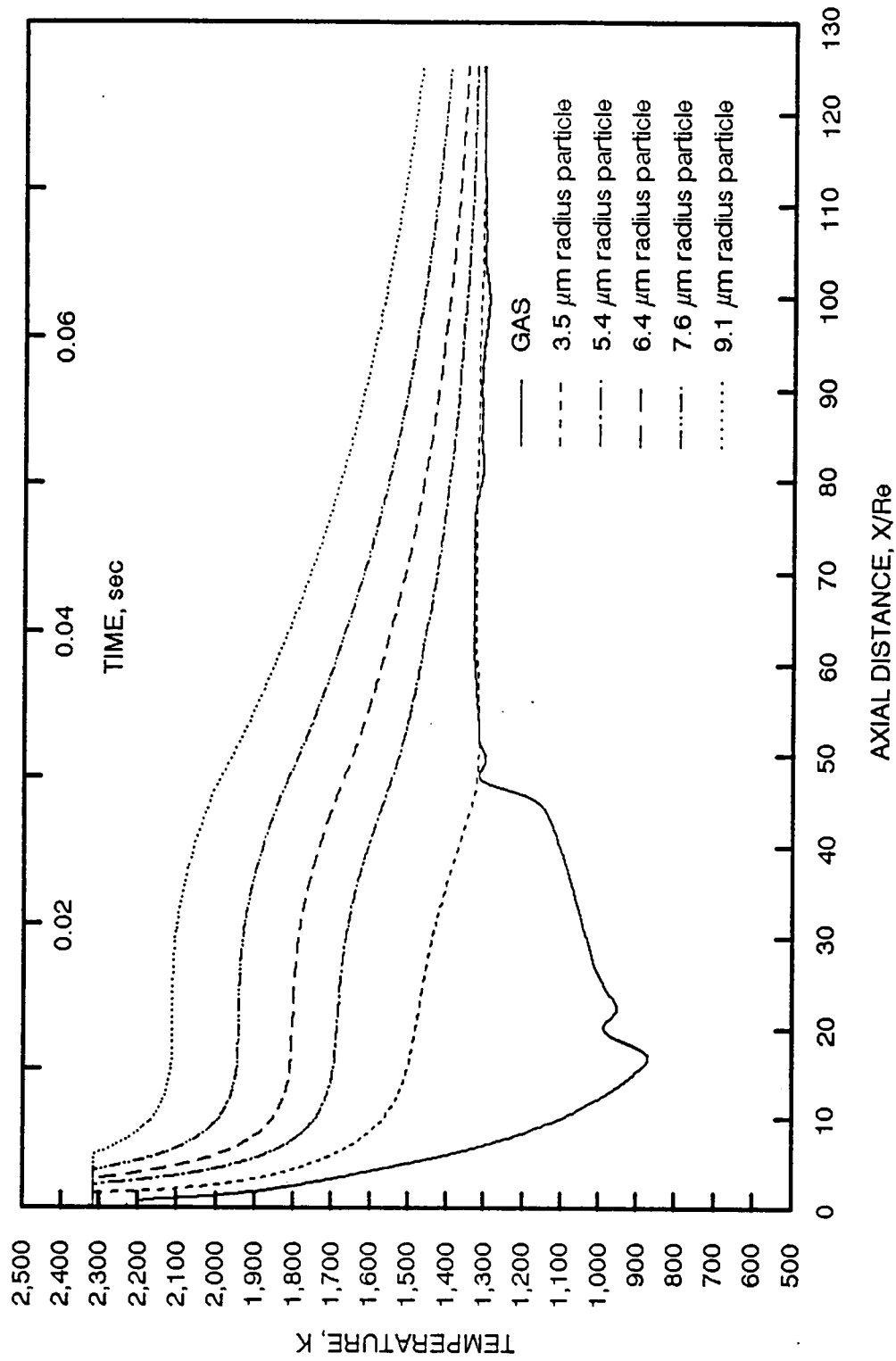
24

Figure 5. ASRM Temperature Profiles at 100,000 ft, Off Centerline, Without Undercooling
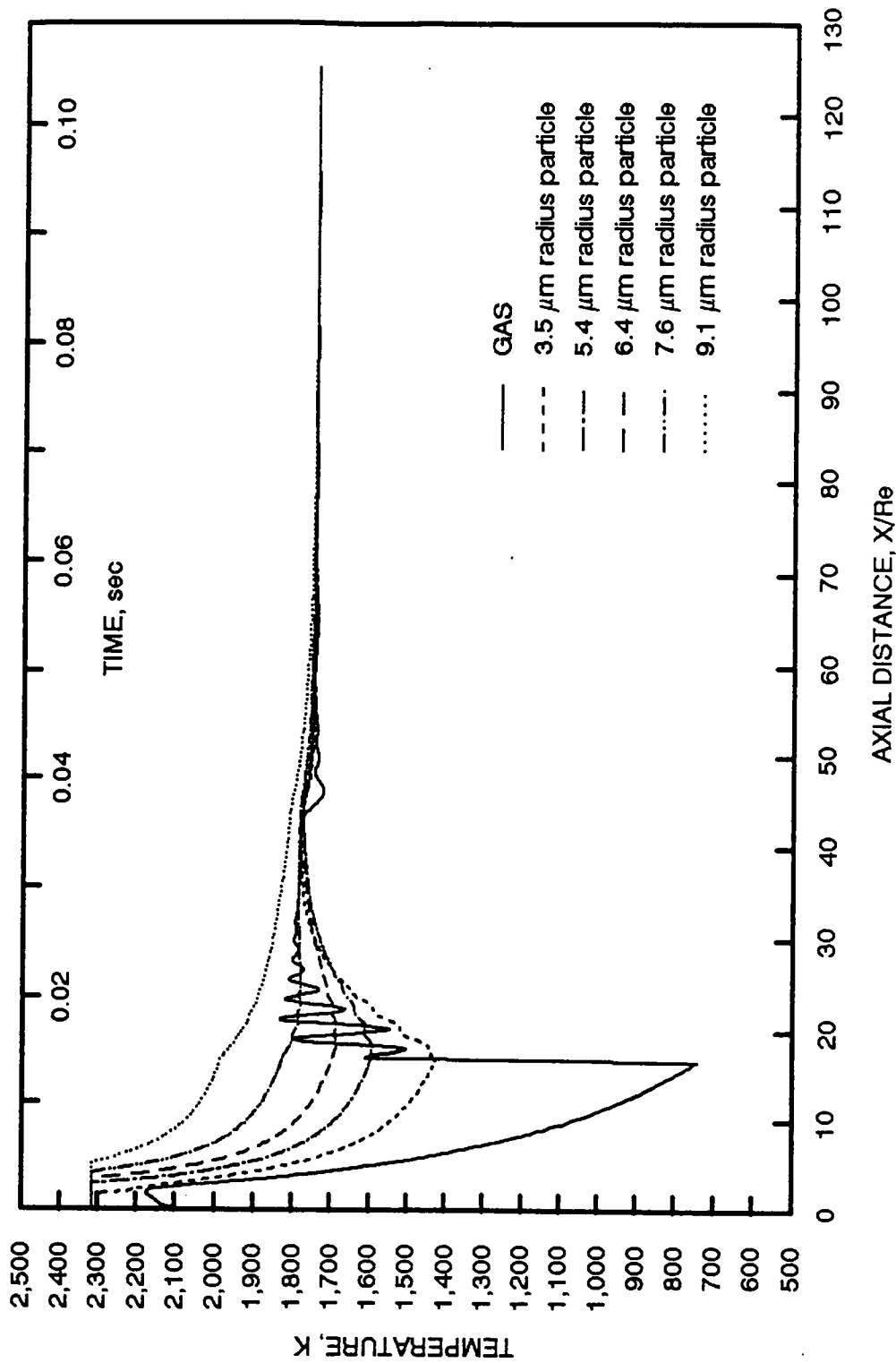
Figure 6. RSRM Temperature Profiles at 100,000 ft, On Centerline, Without Undercooling

distance shown on the lower abscissa. This time was calculated by taking each axial location and dividing it by an average velocity based on the five particle velocities at that location (time = distance/velocity).

The alumina starts out as a liquid droplet and remains liquid until the melt temperature of 2318 K is reached. At this point, the alumina form a two-phase mixture of part liquid and part solid (or "slushball"). The alumina will remain at the plateau temperature of 2318 K until solidification is complete. Once solidification is complete, the particle temperatures continue to decrease.

As shown in Fig. 4, there is a dramatic increase in gas temperature followed by several smaller temperature increases at an axial distance of about 31 nozzle radii (about 194 ft) downstream of the nozzle exit. A similar occurrence is shown in Fig. 6 at a distance of approximately 16 nozzle radii (about 100 ft) downstream. These temperature increases coincide with gasdynamic reflections at these locations. At the location of a reflection, there is a sudden decrease in the Mach number of the gas to a lower supersonic Mach number.

Figs. 4 and 6 show that the gas (the lowest curve) is cooler than the alumina until the reflection point is reached. After the reflection point, there is a jump in gas temperature to a level which exceeds the temperatures of some of the particles. For the off-centerline calculations (Fig. 5), however, the effect of the reflection is not as great, and there is a gradual increase in gas temperature with little or no affect on the particle temperatures. As shown in Fig. 5, the amount of thermal lag

between the gas and the particles increases with particle size. Also, the residence time at which the alumina remain at the 2318 K plateau temperature also increases with particle size.

The gas temperature and the particle temperatures start to converge (Figs. 4-6) after the gas temperature stabilizes at a distance of about 20 to 30 nozzle radii past the reflection location. At an axial distance of 125 nozzle radii (less than 0.1 sec elapsed time), the gas and particle temperatures have not yet begun to decrease to the ambient temperature (approximately 227 K at 100,000 ft) [28]. However, it is expected that at some distance further downstream the gas and particle temperatures would eventually reach the ambient temperature. A sample calculation was performed on the RSRM at 100,000 ft for a distance of 1000 nozzle radii downstream of the nozzle exit. At this distance the gas and particles had still not reached ambient conditions; however, the gas temperature decreased to 900 K on centerline and was several hundred Kelvin cooler just off centerline.

Undercooling

The high end temperature of the droplet temperature-time history is determined by the degree of droplet undercooling prior to solidification which can have a large effect on the final state of the particle. Undercooling (or supercooling) is generally defined as the difference between the melt temperature

(or equilibrium temperature) and the solidification temperature of the droplet [29] and can be expressed as:

$$\text{degree of undercooling} = \text{Tmelt} - \text{Tsolidification} \tag{6}$$

where: Tmelt = the melt temperature of Al_2O_3, K

Tsolidification = the temperature at which the Al_2O_3 begins to solidify, K. For a solidification temperature of 1854 K, the degree of undercooling would be 464 K (2318 K - 1854 K). Thus, the particles would be undercooled by roughly 20 percent since the solidification temperature is approximately 80 percent of the melt temperature. For 20 percent undercooling, the solidification temperature can be calculated by equation 7 [30].

$$\text{Tsolidification(20\%)} = (0.8)(\text{Tmelt}) \tag{7}$$

The maximum degree of undercooling considered in this study was 20 percent. This percentage was based on the results of an experiment by Nelson using free falling molten zirconium oxide droplets [31]. The zirconium oxide data were used because there is no quantitative data for undercooling of Al_2O_3 although undercooling of alumina has often been observed. These results have previously been used as an estimate of undercooling in rocket motors by Henderson [30].

Examples of the effects of droplet undercooling on the droplet temperature-time histories are shown for the ASRM and the RSRM in Figs. 7 and 8 , respectively. The alumina start out as liquid droplets and remain liquid until
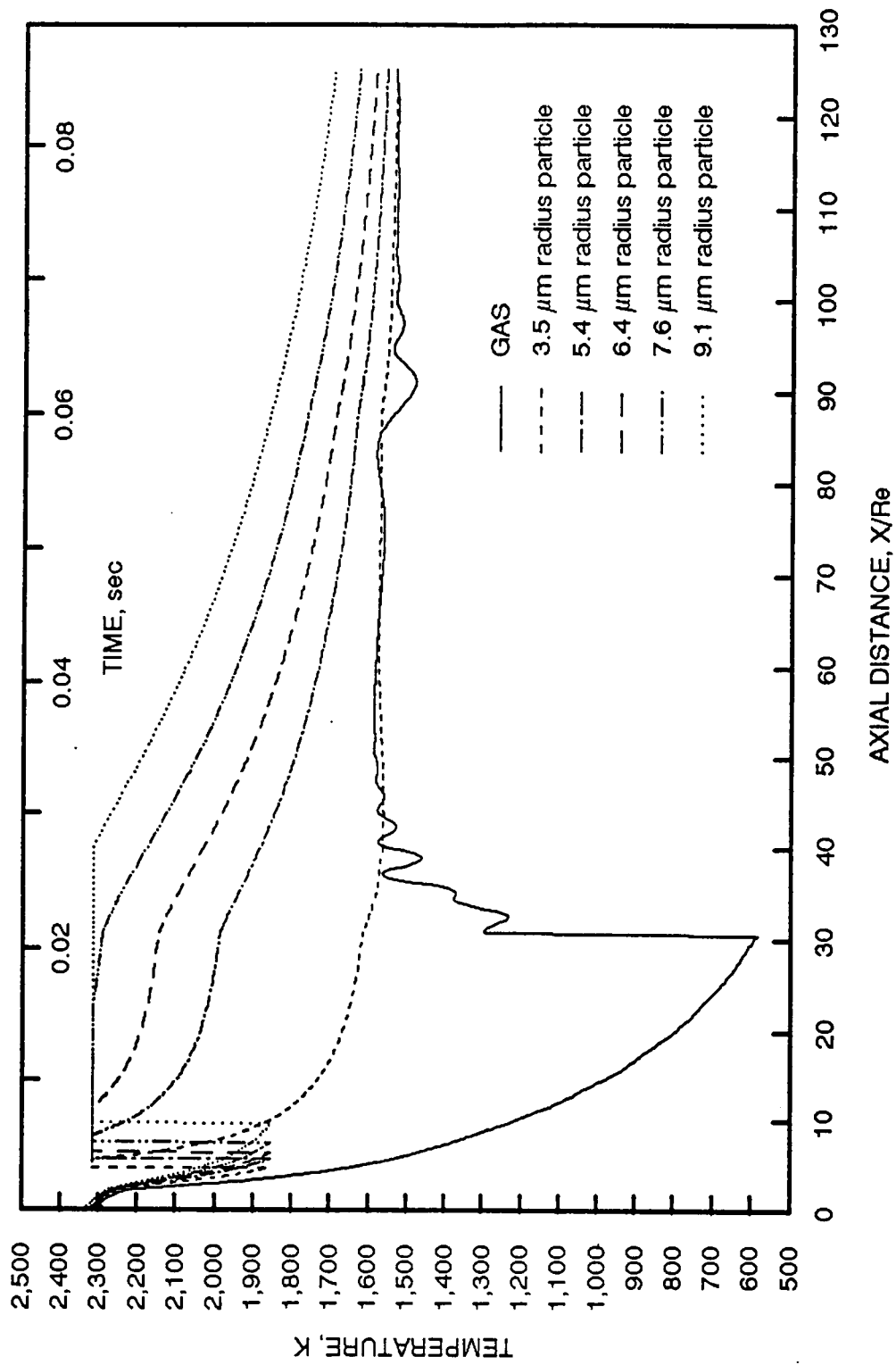
a. Full View of Temperature Profiles

Figure 7. ASRM Temperature Profiles at 100,000 ft, On Centerline, With 20 Percent Undercooling

30
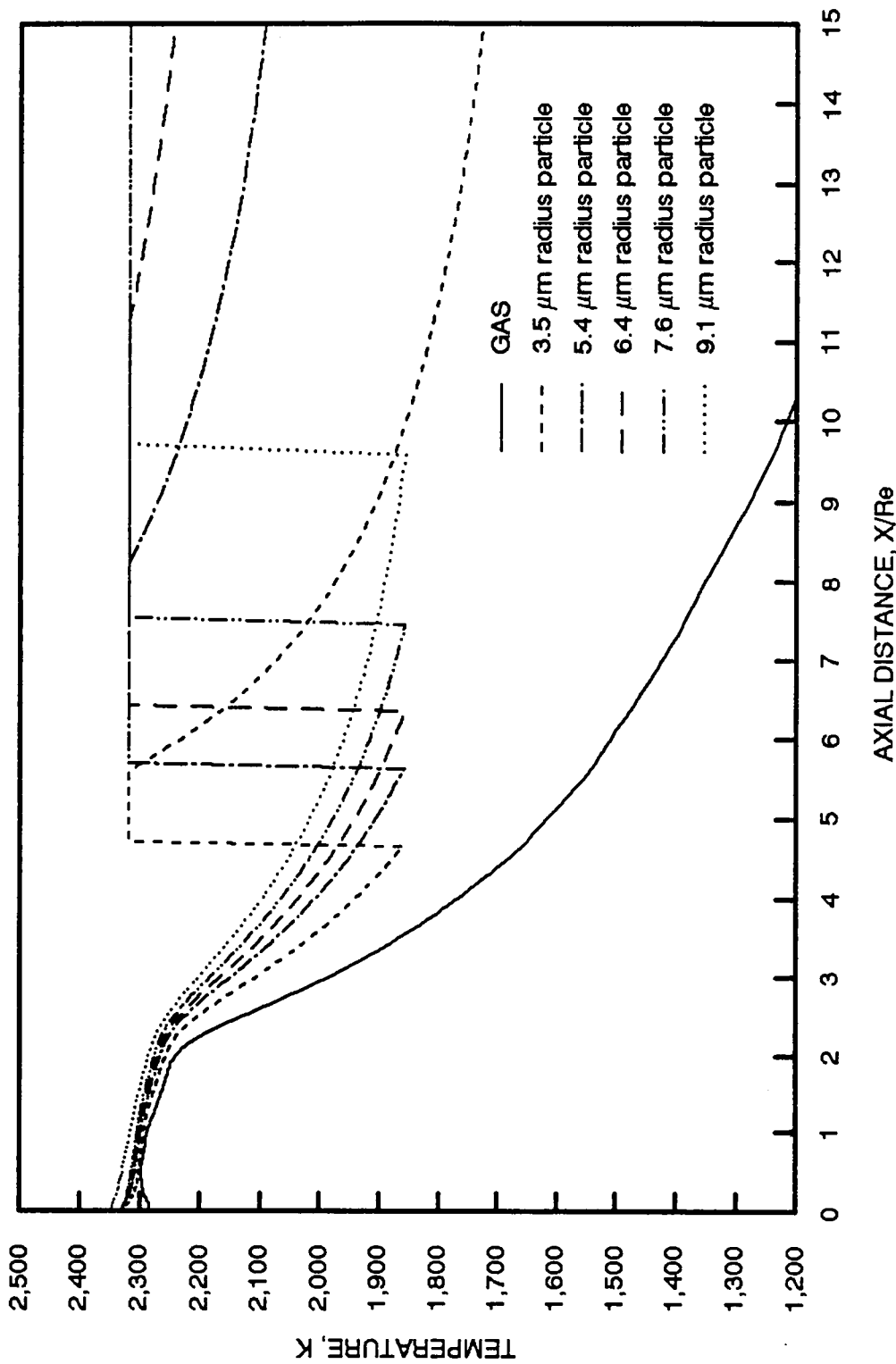
b. Expanded View of Undercooling

Figure 7. Concluded

31

Figure 8. RSRM Temperature Profiles at 100,000 ft, On Centerline, With 20 Percent Undercooling

32

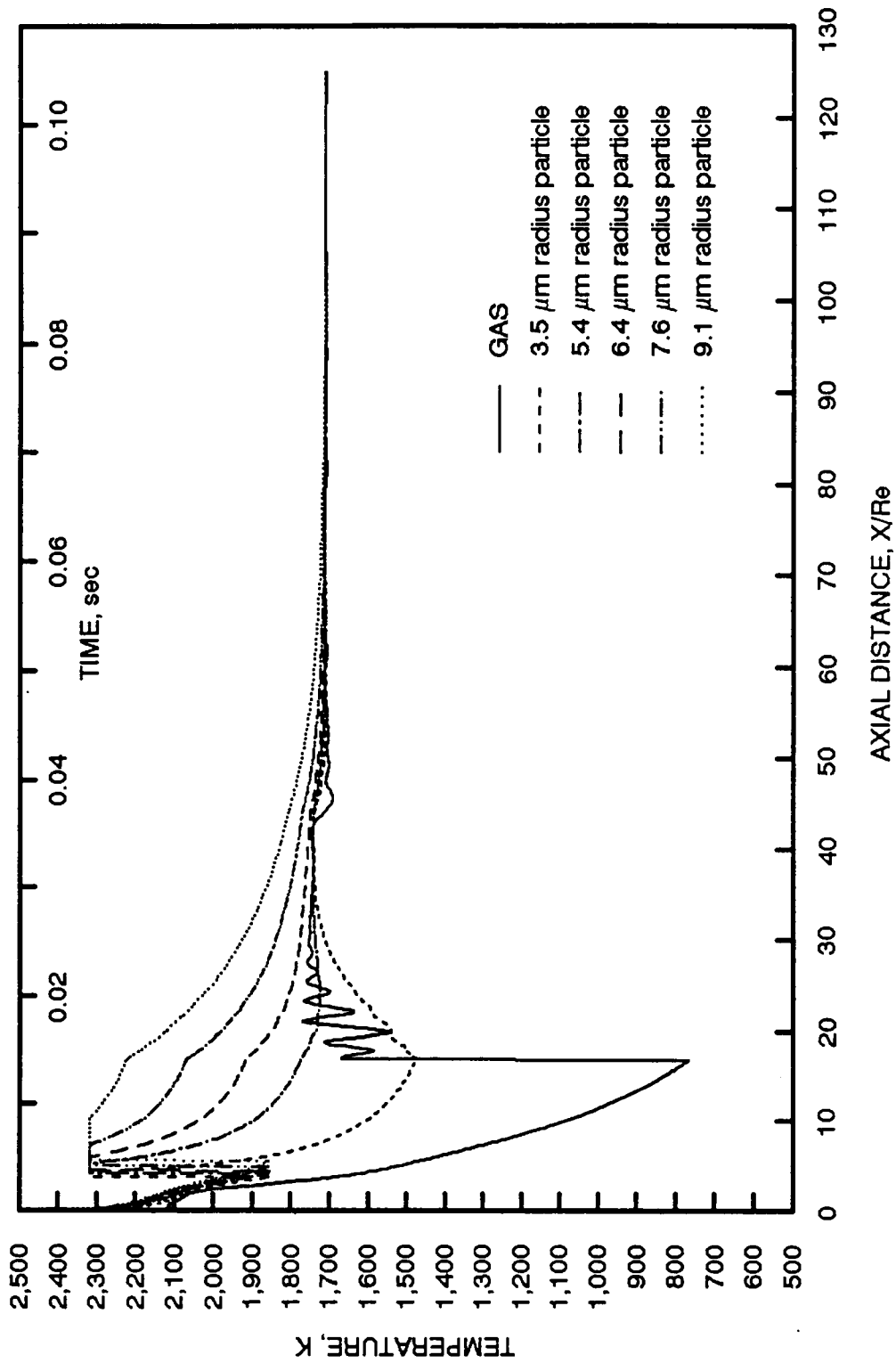reaching a solidification temperature of 1,854 K (which is well below the freezing point of both the alpha and the gamma phases). This solidification temperature was a result of allowing the alumina to undercool by 20 percent. Once the alumina has reached this solidification temperature, there is an abrupt jump in temperature which signals the onset of solidification (Fig. 7b). This occurs because the heat of fusion is being released quicker than it can be dissipated by convection or radiation. The alumina will remain at the 2318 K plateau temperature until solidification is complete.

For the one-dimensional isentropic nozzle flow assumption for a motor with a throat radius of 3.94 in. (10cm) [5], the effect of undercooling on the alpha mass fraction of a 1 μm radius particle was that gamma retention increased as undercooling increased. When no undercooling is present, almost all the alumina are alpha phase. However, as undercooling increases the amount of alpha phase decreases. Thus, for undercooling of 20 percent almost all the gamma is retained. This increase in gamma retention with increase in undercooling is due to the fact that the onset of solidification is shifted to cooler downstream locations where there is faster convective cooling.

For the shuttle calculations, however, the increase in undercooling increased the residence time of the particles at the 2318 K plateau temperature and shifted the solidification closer to the downstream location of the reflection (or

Mach disc) and subsequently hotter temperatures. This increased the amount of gamma to alpha conversion.

Figures 9 and 10 show the alpha mass fraction as a function of undercooling and particle size for both the ASRM and RSRM, respectively. For undercooling greater than five percent, there is an increase in alpha conversion with an increase in undercooling. However, for undercooling less than or equal to five percent, the results are less predictable.

For the RSRM, alpha conversion decreased in all particle sizes except the 5.4 μm radius particle when undercooling increased from zero to five percent. For the 5.4 μm radius particle, alpha conversion increased slightly (one percent). For the case of no undercooling, the 3.5 μm radius particle had more alpha conversion than the 5.4 and 6.4 μm radii particles (21 and 12 percent, respectively). With five percent undercooling, the 3.5 μm radius particle had six and one percent greater alpha conversion than the 5.4 and 6.4 μm radii particles, respectively.

For the ASRM (3.5 μm radius particle, on centerline, 100,000 ft), an increase of undercooling of five percent yielded an increase in alpha conversion of two percent. An increase of ten percent undercooling decreased the alpha conversion by five percent. When undercooling was increased by 15 percent, there was no significant change in alpha conversion. However, an increase of 20 percent undercooling yielded a 12 percent increase in alpha conversion.
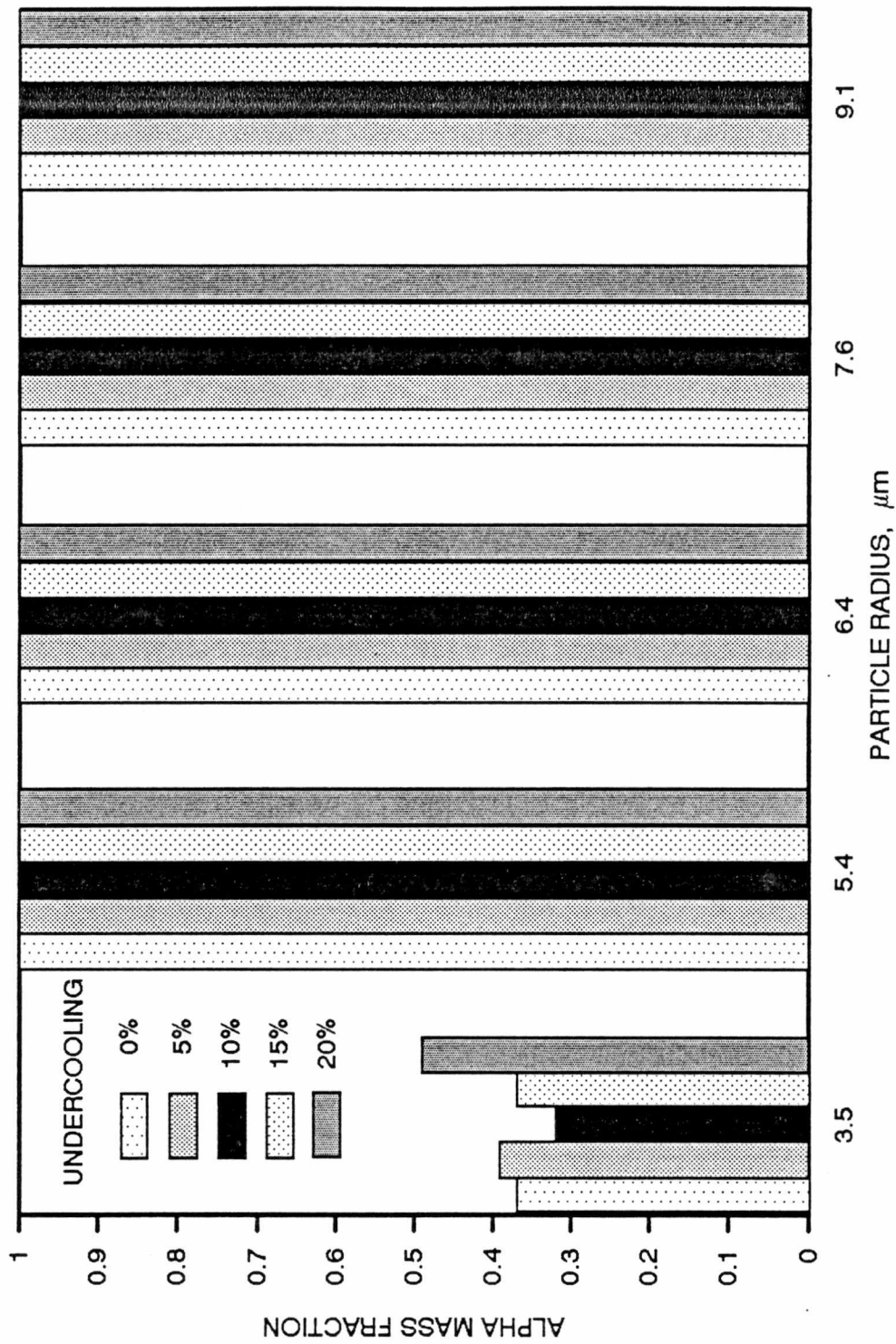
34

Figure 9. ASRM Alpha Mass Fraction as a Function of Particle Size and Percent Undercooling at 100,000 ft, On Centerline
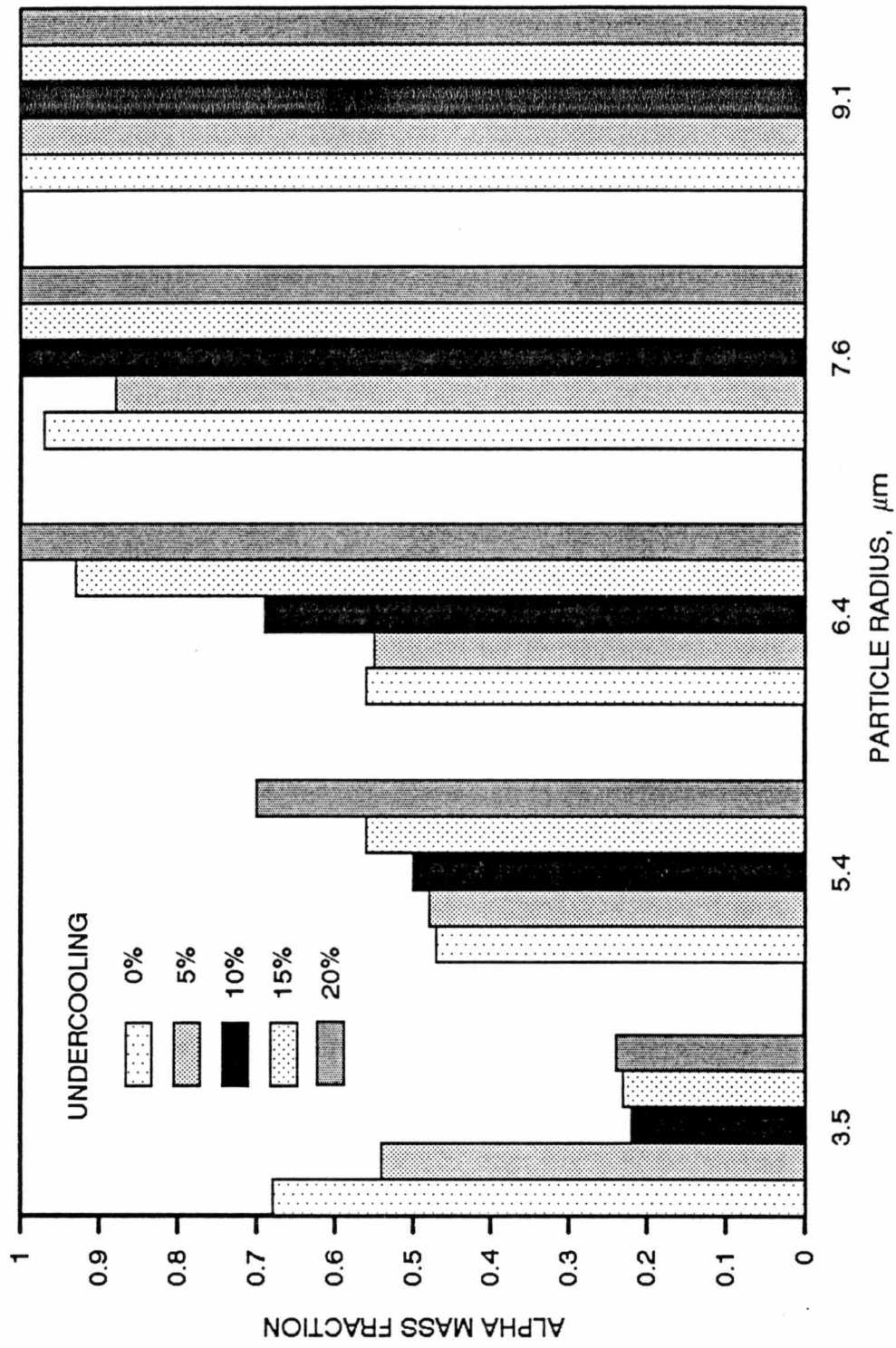
Figure 10. RSRM Alpha Mass Fraction as a Function of Particle Size and Percent Undercooling at 100,000 ft, On Centerline

Particle Size

The extent of gamma to alpha conversion is primarily determined by the residence time of the alumina at the 2318 K plateau temperature. As observed in Figs. 4 and 7, the residence time is a function of particle size and degree of undercooling. For very small particles, the residence time is too short for very much alpha formation to occur. Thus, most of the original gamma is retained. However, for larger particles, the residence time is sufficiently long for most of the gamma to be converted to alpha.

Fig. 11 shows the increase of alpha mass fraction with increasing particle size for the ASRM off-centerline calculation (at an altitude of 100,000 ft and without undercooling). The 3.5 μm radius particle is predominantly gamma while the particles with radii greater than 5.4 μm are predominantly alpha. No correlation with particle size could be made for the ASRM on-centerline calculations (at 100,000 ft. and without undercooling) except that all the particles with radii greater than 3.5 μm converted completely to alpha. The difference in the results in these two calculations can be attributed to the fact that the reflection point does not affect the off-centerline particles as strongly as the particles on centerline. This is evidenced in the temperature profiles shown in Figs. 4 and 5.

Motor Type

The two motors highlighted in this study were the shuttle RSRM and ASRM. Calculations were made for both motors in which particle size and the
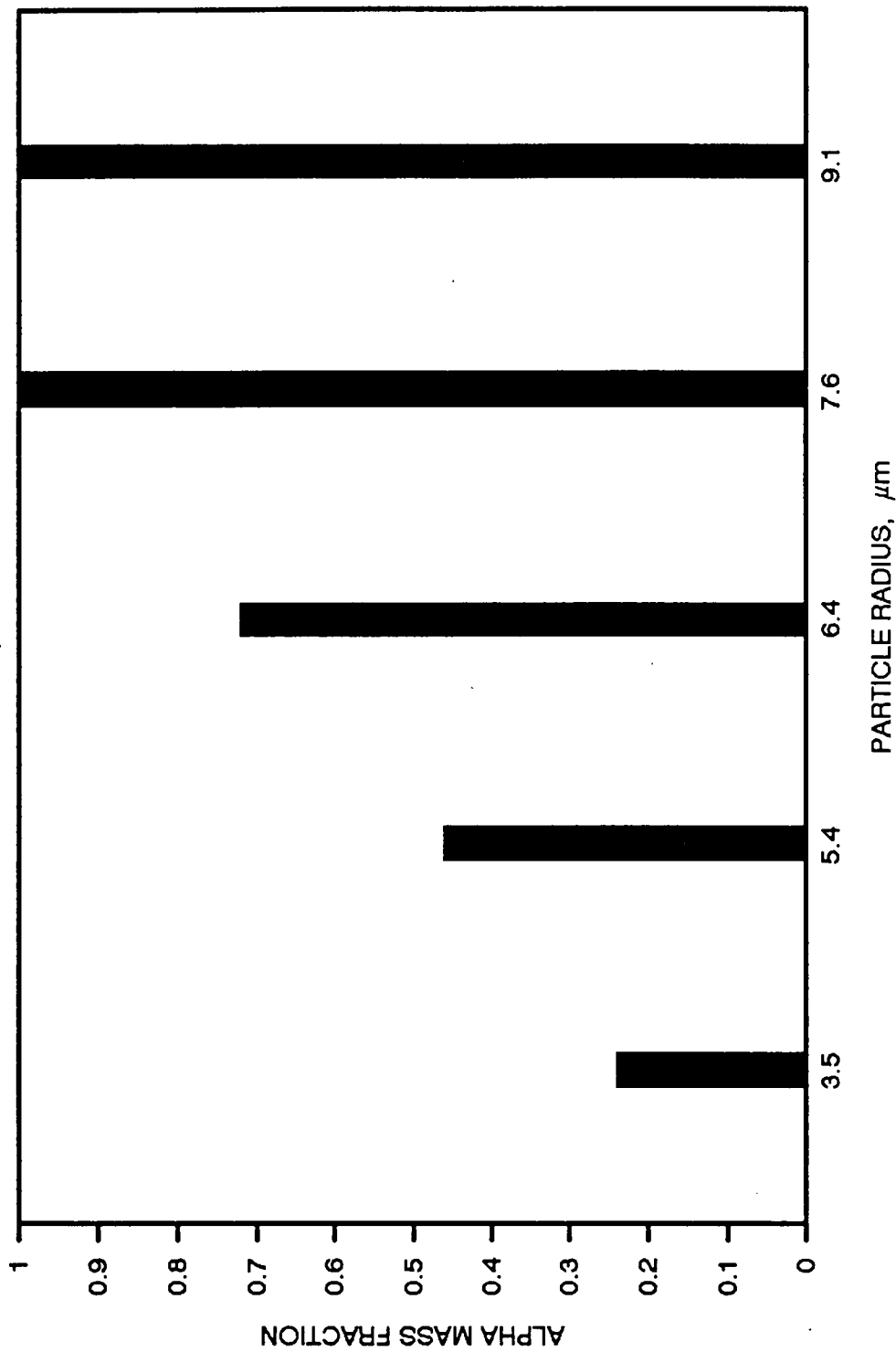
Figure 11. ASRM Alpha Mass Fraction as a Function of Particle Size at 100,000 ft, Off Centerline, Without Undercooling

degree of particle undercooling were varied. These calculations were made on centerline and at an altitude of 100,000 ft. (Additional calculations were made for the ASRM off centerline and at other altitudes.)

The SPF/2 code predictions show that the gas temperature of the ASRM at the nozzle exit is about 180 K higher than that of the RSRM (Fig 4 and 6). This results in longer residence times at the 2318 K melt temperature for most of the ASRM particles and hence less gamma retention. For the on-centerline calculations with undercooling ranging from 0 to 20 percent, all of the ASRM particles with radii greater than 3.5 μm completely converted to alpha.

For the 3.5 μm radius particles, there were greater alpha conversion in the RSRM particles than in the ASRM particles for undercooling of less than or equal to five percent. For undercooling greater than five percent, the reverse was true as shown in Fig. 12.

It should be noted that for the RSRM, the reflection location was about 16 nozzle radii (about 100 ft) downstream of the nozzle exit as compared to the 31 nozzle radii (194 ft) location in the ASRM. As shown in Fig. 6, the gas of the RSRM reaches temperatures higher than most of the particle temperatures at several axial locations (past the reflection location) before the particle temperatures finally converge to the gas temperature.

For motors smaller than the ASRM and RSRM, the one-dimensional calculations [5] indicated that at high altitudes there would not be sufficient time
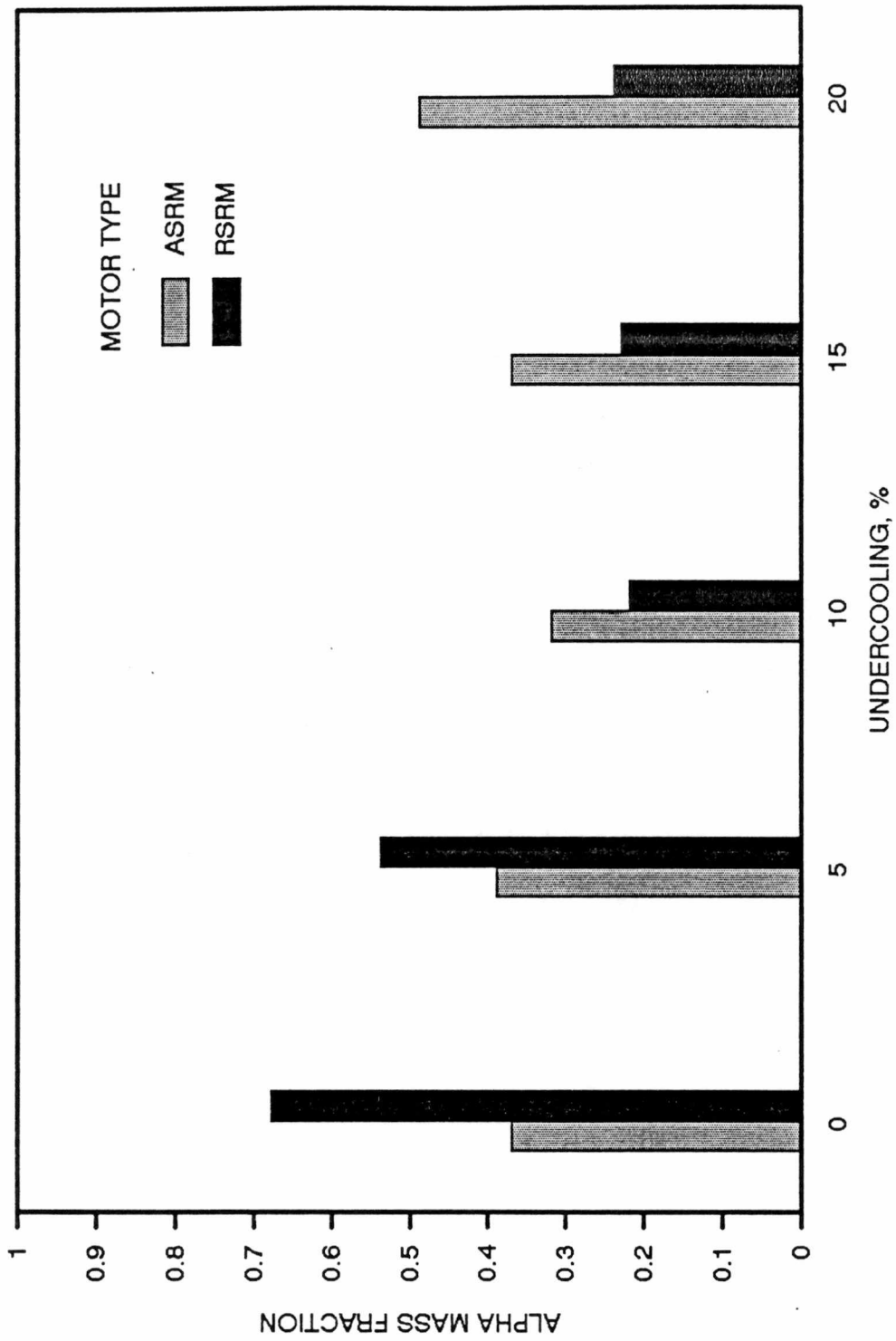
39

Figure 12. ASRM Alpha Mass Fraction as a Function of Motor Type and Percent Undercooling for the 3.5 μm Radius Particle at 100,000 ft, On Centerline

for the exhausted alumina to transform to the alpha phase. In these cases, the particles would be predominantly gamma or one of the other metastable phases. At lower altitudes, however, there is high temperature processing in the plume for extended lengths of time due to afterburning. In these cases, there should be sufficient time for the alumina to transform to the more stable alpha phase [5].

Altitude

Calculations were made for the ASRM at several altitudes. These calculations were made on centerline and without undercooling. The temperature-time histories show that the distance downstream of the nozzle exit at which the reflection (or Mach disc) is located increases with increasing altitude and decreasing motor chamber pressure. The strength of the reflection also varies as evidenced by the temperature increase of the gas following the reflection. Table 4 lists the chamber pressure (Pc), reflection (or Mach disc) location, and change in gas temperature (ΔT) for four altitudes. The gas temperature before the reflection or shock is denoted as T1, and Tmax represents the maximum temperature that the gas reaches after going through the reflection or shock.

At sea level, the reflection was located approximately four nozzle radii (about 25 ft) downstream of the nozzle exit. The gas temperature reached a maximum temperature of 2,682 K. Since the alumina was still liquid at 10 nozzle radii (62 ft), no further calculations were made (Fig. 13).

Table 4. Reflections and Mach Disc Location and Gas Temperature Variation for
Several Altitudes

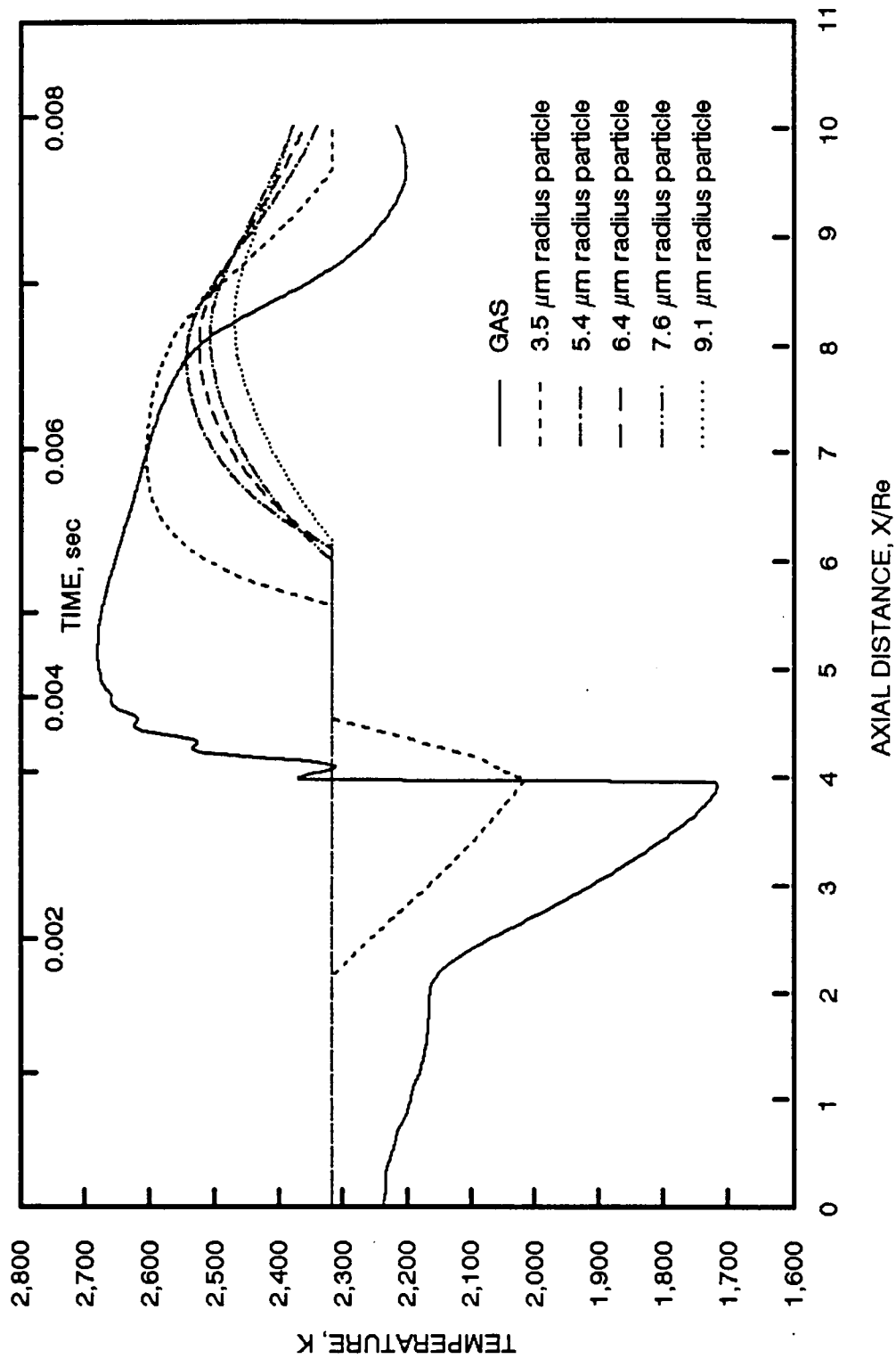| Pc, psia	Location, ft	Altitude, ft	T1, K	ΔT, K	Tmax, K
940	25	Sea Level	1,721	961	2,682
600	94	60,000	910	1,085	1,995
540	193	100,000	600	1,013	1,613
450	349	140,000	300	3,200	3,500

Figure 13. ASRM Temperature Profiles at Sea Level, On Centerline, Without Undercooling

43

At an altitude of 60,000 ft, the reflection was approximately 15 nozzle radii (94 ft) downstream of the nozzle exit. The gas reached a maximum temperature of 1,995 K (Fig. 14) . Since the particles never melted again after solidification, the alpha mass fraction was calculated for each particle size for approximately 125 nozzle radii (780 ft). It was found that there was a large amount of gamma retention in most of the particle sizes upstream of the reflection. However, after passing through the reflection, all particles quickly converted to alpha.

At an altitude of 100,000 ft (Fig. 4), the reflection was located 31 nozzle radii (194 ft) downstream of the nozzle exit. The maximum gas temperature was 1,613 K. The 3.5 μm radius particle had a gamma retention of about 63 percent. All other particle sizes converted completely to alpha. As mentioned earlier, the off-centerline calculation (Fig. 10) at this altitude showed gamma retention in three particle sizes (3.5, 5.4, and 6.4 μm radii).

At an altitude of 140,000 ft, a Mach disc (or shock) was located at approximately 56 nozzle radii (349 ft) downstream of the nozzle exit. The gas flow decelerated from supersonic to subsonic at the Mach disc location. The maximum gas temperature was calculated (using SPF/2) to be 3,500 K (Fig. 15). It should be noted that the actual gas temperature would probably be lower than 3,500 K since the calculations made in SPF are made with the assumption that the chemical properties of the flow are frozen across the shock [13], and the species are not allowed to react. Prior to the location of the Mach disc, all particles were
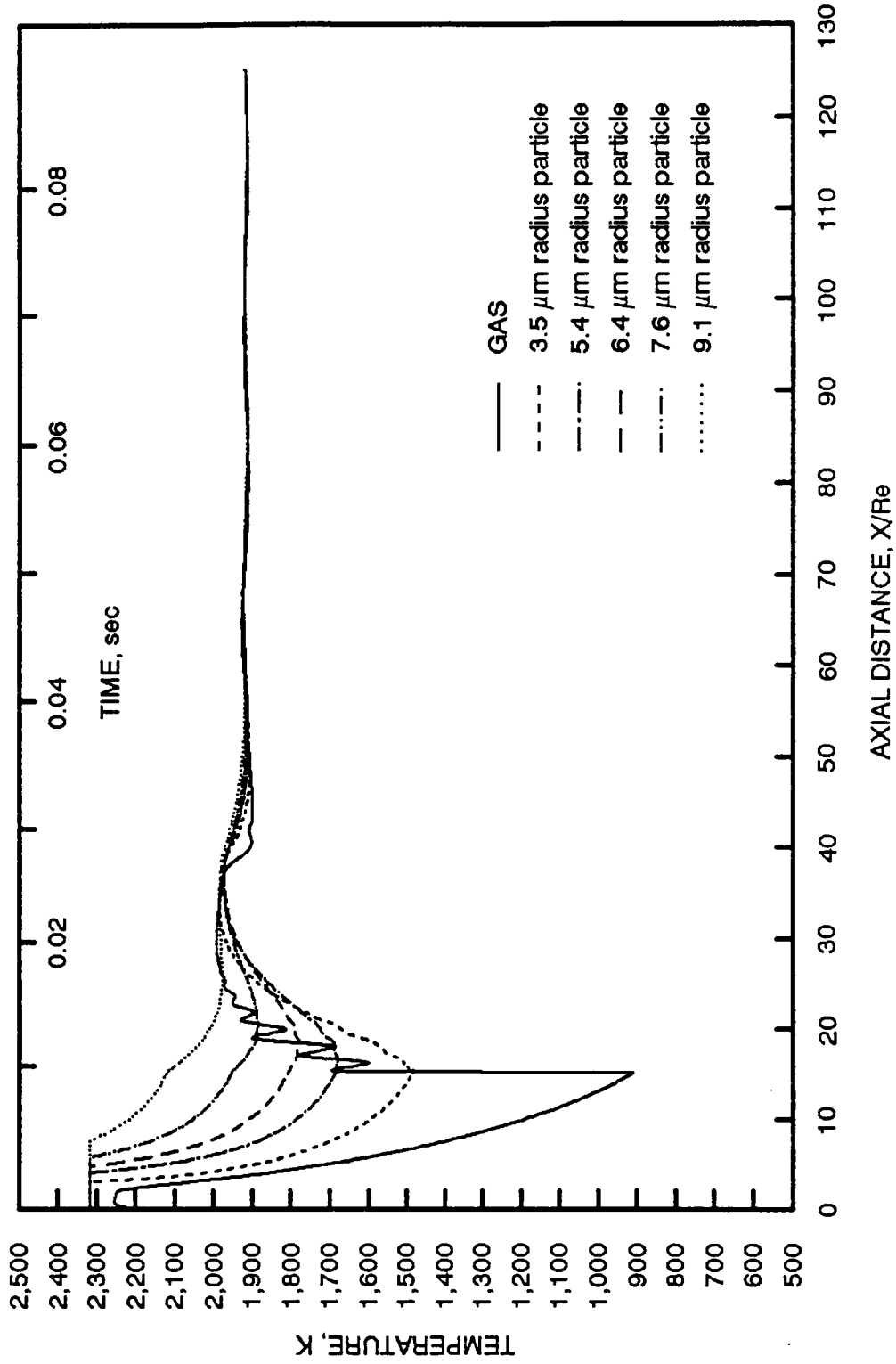
Figure 14. ASRM Temperature Profiles at 60,000 ft, On Centerline, Without Undercooling

45
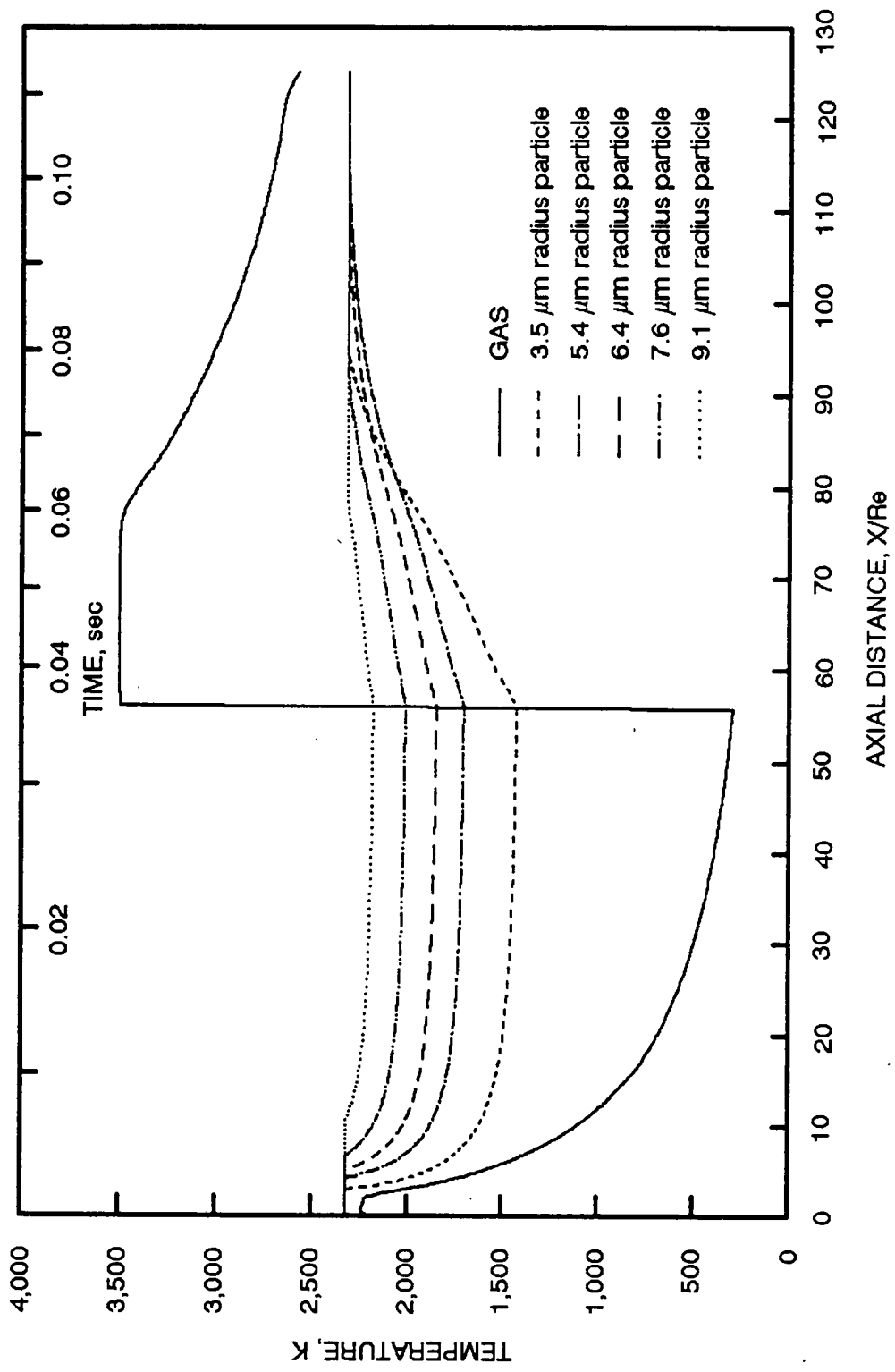
Figure 15. ASRM Temperature Profiles at 140,000 ft, On Centerline, Without Undercooling

solid and at fairly stable temperatures. After the Mach disc, however, all the alumina melted and remained liquid until the end of the calculation (780 ft downstream of the nozzle exit). Since at 780 ft (125 nozzle radii) the gas temperature of 2,581 K was well above the melt point of Al_2O_3, no further calculations were made.

CHAPTER V.

CONCLUSIONS

An analytical approach was developed which calculated the alpha mass fraction of Al_2O_3 particles formed in the exhaust of solid rocket motors which use aluminized propellants. The kinetic rate analysis indicated that significant amounts of metastable aluminas may be formed during the rapid temperature quench often occurring in a gas dynamic nozzle expansion. This study also showed a direct correlation between the alumina crystal phase and particle size, degree of undercooling, motor type, and altitude.

Preliminary calculations were performed [5] for motors smaller than the ASRM and the RSRM with the assumption of one dimensional, isentropic flow nozzle expansion and low aluminum loading. The motors considered had throat radii of 3.94 in. (about 10 cm) or less with thrust of about 100,000 lbf. It was estimated that at high altitudes there would not be sufficient time for the alumina to transform to the alpha phase, and the exhaust particles would be predominantly gamma or one of the other metastable phases. However, at lower altitudes where there is high temperature processing in an afterburning plume for extended lengths of time, there should be sufficient time for the alumina to transform to the more stable alpha phase [5].

Additional calculations were made using an analytical method which utilized the output from industry standard nozzle and plume codes (CEC, RAMP,

48

and SPF/2) as input to a phase conversion code which was based on Steiner's [3] global kinetic rate equation. With this analytical approach, motors with higher aluminum loading and more complex flow fields could be modeled. The nozzle and plume codes were used to model the flow fields for the space shuttle ASRM and RSRM. The particle temperatures and velocities output from these codes were used as input to the phase conversion code which calculated the amount of gamma to alpha conversion for various conditions. On-centerline calculations were made for both motors at an altitude of 100,000 ft with particle sizes varying from 3.5 to 9.1 μm radius and for undercooling varying from 0 to 20 percent. Additional calculations were made for the ASRM at 100,000 ft off centerline and at altitudes ranging from sea level to 140,000 on centerline. The conclusions from these calculations are as follows:

1. PARTICLE SIZE: Generally, the alpha mass fraction increased with increasing particle size. Particles less than 5.4 μm in radius tended to be predominantly gamma while larger particles were predominantly alpha.

2. UNDERCOOLING: For undercooling greater than five percent, the amount of gamma retention decreased with increased undercooling. For undercooling less than or equal to five percent, the results were more erratic and less predictable.

3. MOTOR TYPE: In most cases, the ASRM calculations yielded greater amounts of alpha conversion than the RSRM calculations for all particle

49

sizes. The alpha conversion of the ASRM particles ranged from 10 to 50 percent higher than that of the RSRM particles. The reduction in gamma retention in the ASRM may make it more environmentally safe than the RSRM, but the increase in plume radiance may cause other concerns.

4. ALTITUDE: The ASRM on-centerline calculations showed a slight increase in gamma retention with an increase in altitude from 60,000 ft to 100,000 ft. Other altitudes were considered (sea level and 140,000 ft) but were not pursued when the temperature-time histories indicated that the alumina would remain liquid for extended distances downstream of the nozzle exit.

5. ASRM ON CENTERLINE: For the on-centerline ARSM calculations at an altitude of 100,000 ft, all particles greater than 3.5 µm in radius converted completely to alpha (with and without undercooling).

6. ASRM OFF CENTERLINE: The off-centerline calculations made for the ASRM at an altitude of 100,000 ft indicate that the particles off centerline are not as affected by the reflections which are present in both the ASRM and RSRM plumes. Dramatic decreases in particle and gas temperatures observed in the SPF/2 flowfield calculations at locations just off the centerline also indicate that the centerline results may be atypical of the motor exhaust and that the off-centerline calculations may give a more accurate indication of the gamma to alpha conversion which occurs in these

50

plumes. Also, there was an increase in gamma retention in the off-centerline calculations which means that there may be more metastable alumina present in the ASRM exhausts than indicated by the on-centerline calculations. Additional off-center calculations for both the ASRM and RSRM at various altitudes and degrees of undercooling would be of interest for future studies. A better understanding of the off-centerline flow field is needed before more definite conclusions can be made about the amount of metastable alumina present in SRM plumes.

It has been predicted that significant amounts of metastable alumina will be present in the exhausts of SRM which use aluminized propellants. The amounts of metastable alumina may vary with particle size, undercooling, altitude, and motor type. The presence of metastable alumina is not significant to motor performance, but it may be important in such issues as environmental effects of rocket exhausts, plume radiative heating predictions, and particle size determination by laser scattering. The calculations performed in this study provides some insight into these issues although updated kinetic rate data (based on alumina from SRM exhausts) and actual high altitude measurements of alpha and gamma particles are also needed in order to determine how much metastable alumina are actually present in SRM exhausts.

LIST OF REFERENCES

LIST OF REFERENCES

1. Girata, P. T. and McGregor, W. K., "Particle Sampling of Solid Rocket Motor (SRM) Exhausts in High Altitude Test Cells," AIAA Paper 83-0245, 21st Aerospace Sciences Conference, Reno, Nevada, January 1983.

2. Cofer, W. R., Pellett, G. L., Sebacher, D. I., and Wakelyn, N. T., "Surface Chloride Salt Formation on Space Shuttle Exhaust Alumina," *Journal of Geophysical Research*, Vol. 89, No. D2, pp. 2535-2540, April 20, 1984.

3. Levi, C. G., Jayaram, V., Valencia, J. J., and Mehrabian, R., "Phase Selection in Electrohydrodynamic Atomization of Alumina," *Journal of Materials Research*, Vol. 3, No. 5, pp. 969-983, September/October 1988.

4. Dill, K. M., Reed, R. A., Calia, V. S., and Schulz, R. J., "Analysis of Crystalline Phase Aluminum Oxide Particles from Solid Propellant Exhausts," *AIAA Journal of Propulsion and Power*, Vol. 6, No. 5, pp. 668-671, September-October 1990.

5. Oliver, S. M. and Reed, R. A., "The Kinetics of Alpha vs. Gamma Al_2O_3 Particle Formation in Solid Propellant Rocket Exhausts," AIAA Paper No. 91-0380, 29th Aerospace Sciences Meeting, Reno, Nevada, January 1991.

6. French, R. H., "Electronic Band Structure of Al_2O_3, with Comparison to ALON and ALN," *Journal of the American Ceramic Society*, Vol. 73, No.3, pp. 477-489, March 1990.

7. McDonald, A. J., Bennett, R. R., Hinshaw, J. C., and Barnes, M. W., "Chemical Rockets and the Environment," *Aerospace America*, Vol 29, No. 5, pp. 33-36, May 1991.

8. Aftergood, S., "Poisoned Plumes," *New Scientist*, Vol. 131, No. 1785, pp. 34-38, September 1991.

9. Nebergall, W. H., Holtzclaw, H. F., and Robinson, W. R., *College Chemistry*, Lexington, Massachusetts, D. C. Heath and Company, pp. 923-924, 1980.

10. Cofer, W. R., Lala, G. G., and Wightman, J. P., "Analysis of Mid-Tropospheric Space Shuttle Exhausted Aluminum Oxide Particles," *Atmospheric Environment*, Vol 21, No. 5, pp. 1187-1196, 1987.

11. Keller, V. W., *Ice Nuclei Activity Measurements of Solid Rocket Motor Exhaust Particles*, NASA-TM-8655, September 1986.

12. Moylan, B., *Final Report for the Solid Rocket Plume Radiation Prediction Analysis*, NASA Report TD 631-002-05, November 30, 1990.

13. Dash, S. M. and Pergament, H. S., "A Computational System for the Analysis of Mixing/Chemical/Shock Processes in Supersonic Internal and Exhaust Plume Flowfields," AIAA Paper No. 80-1255, 16th AIAA/SAE/ASME Joint Propulsion Conference, Princeton, N. J., July 1980.

14. Steiner, C. J-P., Hasselman, D. P. H., and Spriggs, R. M., "Kinetics of the Gamma-to-Alpha Alumina Phase Transformation," *Journal of the American Ceramic Society*, Vol. 54, No. 8, pp. 412-413, August 1971.

15. Moeller, T., Bailar, J. C., Kleinberg, J., Guss, C. O., Castellion, M. E., and Metz, C., *Chemistry with Inorganic Qualitative Analysis*, New York, New York, Academic Press, Inc., p. 808, 1980.

16. Whitney, T., Jayaram, V., Levi, C. G., and Mehrabian, R., "Rapid Solidification of Alumina-Zirconia Eutectic and Hypoeutectic Alloys," *Solidification Processing of Eutectic Alloys*, The Metallurgical Society, pp. 199-216, 1988.

17. Fyfe, W. S., *Geochemistry of Solids: An Introduction*, New York, McGraw-Hill Book Company, pp. 104-106, 1964.

18. Mackowiak, J., *Physical Chemistry for Metallurgists*, New York, American Elsevier Publishing Company, Inc., pp. 196-229, 1966.

19. Tucker, D. S. and Hren, J. J., "The $\gamma \rightarrow \alpha$ Phase Transformation in Al_2O_3," *Materials Research Society, Symp. Proc.*, Vol. 31, 1984.

20. Bye, G. C. and Simpkin, G. T., "Influence of Cr and Fe on Formation of α-Al_2O_3 from γ-Al_2O_3," *Journal of the American Ceramic Society*, Vol. 57, No. 3, pp. 367-371, August 1974.

21. Iler, R. K., "Fibrillar Colloidal Boehmite; Progressive Conversion to Gamma, Theta, and Alpha Alumina," *Journal of the American Ceramic Society*, Vol. 44, No.12, pp. 618-624, December 1961.

22. Dynys, F. W. and Halloran, J. W., "Alpha Alumina Formation in Alum-Derived Gamma Alumina," *Journal of the American Ceramic Society*, Vol. 65, No.9, pp. 442-448, September 1982.

23. McDonald, A. J., "Fixing the Field Joint That Failed on the Challenger," *Journal Propulsion and Power*, Vol. 7, No. 2, March-April 1991.

24. Bardos, R., "Shuttle Propulsion Systems," *Space Transportation Propulsion Technology Symposium, Vol. 2 - Symposium Proceedings*, NASA CP-3112, Vol. 2, pp. 151-166, May 1991.

25. George, D., "Recent Advances in Solid Rocket Motor Performance Prediction Capability," AIAA Paper No. 81-0033, 19th Aerospace Sciences Meeting, St. Louis, Missouri, January 1981.

26. Gordon, S. and McBride, G. B., *Computer Program for the Calculation of Complex Chemical Equilibrium Compositions, Rocket Performance, Incident and Reflected Shocks, and Chapman-Jouguet Detonations*, NASA SP-273, March 1976.

27. Smith, S. D., SECA Inc., Private communication.

28. White, F. M., *Fluid Mechanics*, New York, New York, McGraw-Hill Book Company, p. 680, 1979.

29. Fisher, W. K., *Fundamentals of Solidification*, Third Edition, Switzerland, Trans Tech Publications, p. 22, 1989.

30. Henderson, C. B., "Effect of Crystallization Kinetics on Rocket Performance," *AIAA Journal*, Vol. 15, No. 4, pp. 600-602, April 1977.

31. Nelson, L. S., "Possible Role of Supercooling in the Spearpoints Observed During the Combustion of Zirconium Droplets," *Nature*, Vol. 210, pp. 410-411, April 23, 1966.

VITA

Suzanne Moore Oliver was born on October 12, 1953 in Atlanta, Georgia to John and Rosalie Moore. She graduated from Tullahoma Senior High School in 1971 and attended Motlow Community College full time for one year. Ms. Oliver worked as a bookkeeper for several years and attended Motlow part time until receiving a two year cooperative (co-op) education assignment as an engineering trainee with the Air Force at Arnold Engineering Development Center (AEDC) in the turbine engine section of the Directorate of Propulsion (DOPT).

She graduated Summa Cum Laude from Motlow Community College in June 1983. In the fall of 1984, she enrolled at Tennessee Technological University. She served as Vice-President and President of the Tau Beta Pi Engineering Honor Society and was active in several other engineering and academic organizations until her graduation in June 1986.

Ms. Oliver began employment with Sverdrup Technology, Inc. in June 1986. She currently is assigned as a Project Manager and Work Element Manager in the Advanced Propulsion Diagnostics Section in the area of plume diagnostics.

Ms. Oliver enrolled at the University of Tennessee Space Institute (UTSI) in September 1986 and completed her course work in May 1990. She received a Master of Science degree in Mechanical Engineering in December 1991.